

## ORIGINAL ARTICLE

# The potential of a canister-based single-use negative-pressure wound therapy system delivering a greater and continuous absolute pressure level to facilitate better surgical wound care

Aleksei Orlov | Amit Gefen 

Department of Biomedical Engineering,  
Faculty of Engineering, Tel Aviv  
University, Tel Aviv, Israel

**Correspondence**

Amit Gefen, Department of Biomedical  
Engineering, Faculty of Engineering, Tel  
Aviv University, Tel Aviv 6997801, Israel.  
Email: [gefen@tauex.tau.ac.il](mailto:gefen@tauex.tau.ac.il)

**Funding information**

H2020 Marie Skłodowska-Curie Actions,  
Grant/Award Number: 811965; project  
STINTS (Skin Tissue Integrity under  
Shear); Ministry of Science, Technology  
and Space, Grant/Award Number:  
Medical Devices Program Grant  
no. 3-17421; Mölnlycke Health Care  
(Gothenburg, Sweden)

**Abstract**

Two types of single-use negative-pressure wound therapy systems are currently available to treat surgical wounds: Canister-based and canisterless. This work was aimed to evaluate the performance of a canister-based vs a canisterless system, each with a different negative-pressure setting and technology for fluid management. Continuous delivery of a specified level of negative pressure to the wound bed is hypothesised to be important for promoting surgical wound healing, by achieving continuous reduction of lateral tension in the wound, particularly through decrease of skin stress concentrations around suture insertion sites. To test the above hypothesis, we developed a computational modelling framework, a laboratory bench-test for simulated clinical use and had further conducted a pre-clinical study in a porcine model for closed incision. We specifically focussed on the impact of effective fluid management for continuous delivery of a stable, consistent negative pressure and the consequences of potential losses of the pressure level over the therapy period. We found that a greater (absolute) negative-pressure level and its continuous, consistent delivery through controlled fluid management technology, by removing excess fluid from the dressing, provides far superior biomechanical performances. These conditions are more likely to result in better quality of the repaired tissues.

**KEYWORDS**

animal study, bioengineering laboratory research, closed incision, finite element modelling, lateral tension sutures

**List of Abbreviations:** ANOVA, analysis of variance; CB, canister-based; CL, canisterless; FE, finite element; LSD, long suturing distance; NPWT, negative pressure wound therapy; PBS, phosphate-buffered saline; SDD, stress-dose difference; SPP, skin perfusion pressure; SSD, short suturing distance; su, single-use; USP, United States Pharmacopeia; UTS, ultimate tensile strain.

This is an open access article under the terms of the [Creative Commons Attribution-NonCommercial-NoDerivs](https://creativecommons.org/licenses/by-nc-nd/4.0/) License, which permits use and distribution in any medium, provided the original work is properly cited, the use is non-commercial and no modifications or adaptations are made.

© 2021 The Authors. *International Wound Journal* published by Medicalhelplines.com Inc (3M) and John Wiley & Sons Ltd.

### Key Messages

- single-use negative-pressure wound therapy systems are used postoperatively
- clinicians can choose between canister-based vs canisterless system types
- computer model, laboratory tests and porcine model compared these system types
- a system supplying greater (absolute) negative-pressure level is advantageous
- controlled fluid management is vital for consistent pressure therapy course

## 1 | INTRODUCTION

Negative-pressure wound therapy (NPWT) has revolutionised the treatment of acute and chronic wounds since it was introduced in the late 20th century.<sup>1,2</sup> When used on closed surgical incisions, the specific beneficial modes of action of NPWT include promotion of perfusion, lower oedema, seroma and hematoma and reduction of dead spaces and lateral tissue stresses by holding the wound edges of the incision together.<sup>3-5</sup> Application of NPWT can be considered for a variety of wound etiologies and treatment stages.<sup>6-9</sup> Traditional NPWT systems are designed to be stationary and function for several years, during which they serve a large number of patients.<sup>10</sup> These systems, which remain commercially available, are always *canister-based* (CB). Traditional NPWT systems are therefore mostly used for inpatients or require frequent hospital visits, which may compromise the quality of life of patients.<sup>9,11,12</sup> A modern approach has been the development of portable, single-use (su)NPWT systems suitable for treating the wounds of outpatients. These require less or no maintenance, are simple to operate and consume less expert clinician time, contributing to a cost-benefit advantage. Single-use NPWT systems further facilitate a daily living routine and promote mobility and physical activity, which reduces the risks for stroke or hypertension.<sup>9,10,12,13</sup>

Currently, there are two commercially available types of suNPWT systems: CB and *canisterless* (CL), also known as ‘canister-free’. Both types of systems manage wound exudates through a multilayer wound dressing, which is connected to a pump unit by a tube for creating the negative pressure in the wound bed via the dressing. In CL systems, the fluid is managed only by the dressing, rendering CL systems dependent on the moisture vapour transmission rate of the dressing for fluid management. In CB systems, however, fluid from the wound is managed between the dressing and a canister, which collects excess exudate and infectious substances. This results in consistent therapy over time, where the intended negative pressure delivered to the wound bed is

uncompromised by fluid retention in the dressing. Both types of suNPWT systems are indicated for application on either chronic or acute wounds<sup>9,11,14,15</sup> and have become especially popular in postoperative use.<sup>16,17</sup>

Primary closure of surgical incisions, particularly of large ones, by means of sutures, involves a risk for serious post-surgical complications such as infections but also, complications caused by the localised, intense forces of the sutures that act on the peri-wound skin. Such reported complications may include skin and adipose necrosis, which are conducive to infections and may further lead to considerable scarring.<sup>18,19</sup> In this clinical context, we hypothesise here that the continuous action of suNPWT may aid the healing of surgical wounds, by reducing the lateral tension along the incision line and, particularly, the levels of the mechanical stress concentrations around the suture sites (Figure 1).<sup>20</sup>

Although computational finite element (FE) modelling has been used extensively to investigate the effects of various medical devices on tissue function, including, as in our own work, to study the roles of NPWT in wound closure,<sup>20-23</sup> very little research has been published on specifically modelling surgical incisions treated by NPWT. Wilkes and colleagues<sup>24</sup> who modelled a two-dimensional cross-sectional geometry of a closed incision managed through NPWT and Loveluck et al<sup>25</sup> who similarly simulated a thin-slice of a surgical incision treated by NPWT only considered the in-plane mechanical effects of NPWT in their respective FE models. In addition, these two studies did not account for the actual presence of suture materials in skin and further employed a simplified, hyperelastic representation for simulating the soft tissue behaviours, which are viscoelastic in nature. Importantly, none of the above published studies considered the influence of the different fluid management technologies, that is, the CB vs CL suNPWT systems, on the efficacy of the applied NPWT system to continuously deliver the intended negative pressure and, thereby, provide consistent therapy.

In this work, we report a comprehensive study aimed at testing the above hypothesis (Figure 1), by means of an

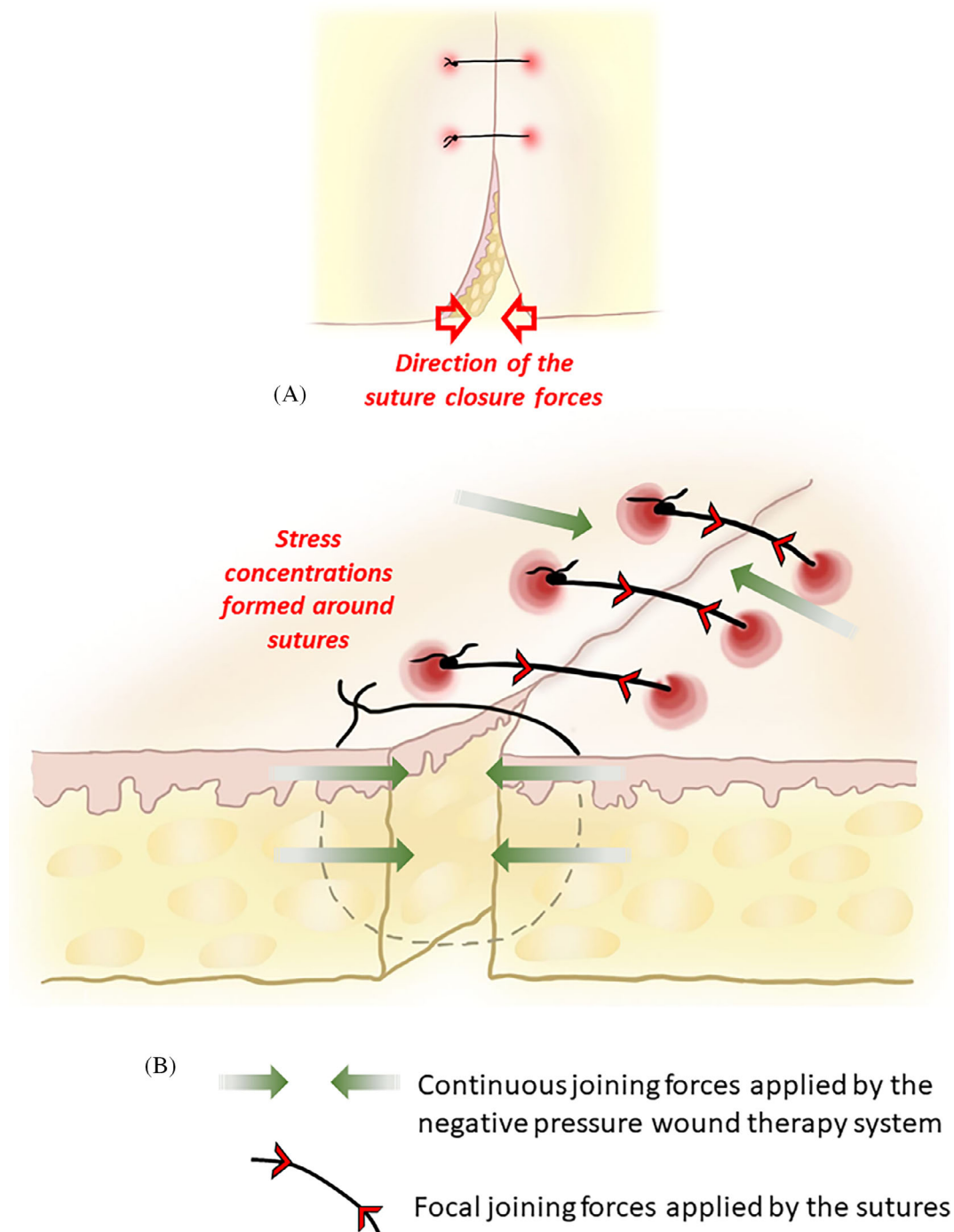


**FIGURE 1** Closure of a surgical incision: (A) Primary closure of the wound using the simple interrupted suturing technique (top view) and (B) a conceptual description of the force distribution after the closure of a surgical incision using suturing followed by application of a negative-pressure wound therapy

integrated bioengineering approach with empirical laboratory investigations, FE modelling and a wound healing study in a porcine model for closed incisions. We focussed our research efforts on understanding the biomechanical implications of selecting and using a CB, as opposed to a CL suNPWT system, given their different technologies for fluid management. In particular, we

evaluated the influence of the level and stability of the negative pressures delivered by these systems on the tissue loading state in the wound vicinity. We determined how these factors affect the reduction of stress concentrations in peri-wound skin around the sutures, as these skin stress concentrations were previously suggested to impact the clinical outcome of the closure.<sup>20</sup>

## 2 | METHODS

### 2.1 | Performance tests under conditions of simulated clinical use

Laboratory bench-tests under conditions that simulate clinical use were conducted to determine whether a CL suNPWT system, as compared to a CB suNPWT system, would have capacity to maintain delivery of the intended negative-pressure level to the wound bed as the wound fluid progressively saturates the dressing. To test the above hypothesis, a wound model (made of Plexiglass/Perspex) simulating the application of NPWT, and applying horse serum\* as the exudate simulant, was set up. The flow rate of this simulated wound fluid, expressed as gram fluid per  $\text{cm}^2$  wound area during 24 hours, was set to represent a low ( $0.6 \text{ g/cm}^2$  wound area/24-hours) and a moderate ( $1.1 \text{ g/cm}^2$  wound area/24-hours) exuding wound. The test time was set to 4 days (96 hours) or 3 days (72 hours), respectively,<sup>26,27</sup> to reflect the recommended dressing change frequency in actual use.

The suNPWT dressings used throughout this study are breathable, multilayer wound dressings designed with an absorptive core, a distribution layer that transmits negative pressure evenly over the dressing and a protective wound contact layer. The fluid was delivered from underneath the tested dressings, using a calibrated peristaltic pump with a controlled fluid outlet. Delivery of negative pressure from the suNPWT pump to the simulated wound bed was measured and sampled every 60 seconds using differential pressure transmitter sensors (model KIMO CP214-BNs, Kimo Instrument Sverige AB, Gothenburg, Sweden), operating between  $-500$  and  $500$  mbar, which were positioned to measure the pump output of negative pressure to the dressing and its pressure delivery at multiple positions under the dressing in the simulated wound bed. These pressure sensors were sampled via a NI-DAQmx control unit and a custom-made LabVIEW software code (National Instruments, Austin, Texas), and all pressure measurements were digitally recorded for offline analyses. The evaluation measuring the negative-pressure delivery through the suNPWT system at specific levels of saturation of the dressing represented treatment of an exuding wound for a minimum of 3 day application of the suNPWT system (Figure 2). Before the tests, the dressings were subjected to a volume of exudate simulant corresponding to 20%, 40%, 60% and 80% of the expected wound fluid volume when applied on a moderately exuding wound for an application time of at least 72 hours (which is the recommended frequency for dressing changes in a clinical setting). The test was performed for both the CB and CL

suNPWT systems, with five replicates ( $N = 5$ ) at each dressing saturation level.

### 2.2 | Computational study

#### 2.2.1 | Geometry of the model and the mechanical properties of its components

We have modelled an elliptically shaped surgical incision with skin surface-plane dimensions of  $50 \times 2 \text{ mm}$  (length  $\times$  width) that extends to a depth of 7 mm into the subepidermal adipose tissue (Figure 3A). We further simulated primary closure by suturing, followed by application of a suNPWT system. An interrupted suture technique has been modelled in two configurations: long suturing distance (LSD) and short suturing distance (SSD) with 5 and 9 sutures, respectively (Figure 3B). The soft tissue model with the incision wound comprised of four layers: epidermis, dermis (together referred to as 'skin'; Figure 3A), adipose and underlying skeletal muscle with thicknesses of 1, 2, 8 and 12 mm, respectively<sup>28</sup> (Figure 3A). The dressings of both the CB and CL suNPWT systems were modelled as a single rectangular layer of wound pad with dimensions of  $80 \times 30 \times 5 \text{ mm}$  (length  $\times$  width  $\times$  height). The dressing was initially positioned 0.5 mm above the incision (to be able to simulate the process of its application on the wound, as explained further), so that the longest aspect of the wound pad was aligned with the widest dimension of the incision, which resulted in that the dressing covered the entire incision after application, as would have been done clinically (Figure 3A). Sutures were modelled as cylinders that penetrate the entire depth of the skin with dimensions of  $3 \times 0.25 \text{ mm}$  (height  $\times$  radius) (Figure 3A). The overall model dimensions (ie, the geometrical model domain) were  $300 \times 300 \times 23 \text{ mm}$  (length  $\times$  width  $\times$  height), which leaves substantial margins around the surgical incision site to avoid potential boundary effects according to Saint-Venant's principle. The above geometry of the model domain (Figure 3A) was created using the Scan-IP module (R – 2020.09) of the Simpleware software package (Synopsys Inc., Mountain View, California).<sup>29</sup> The mechanical behaviour and properties of each of the model components are detailed in Appendix A.1.

#### 2.2.2 | Boundary and loading conditions in the computational modelling

The side faces of the model were fixed for all translations and rotations, to consider the continuum interactions of the included soft tissues with tissues outside the model

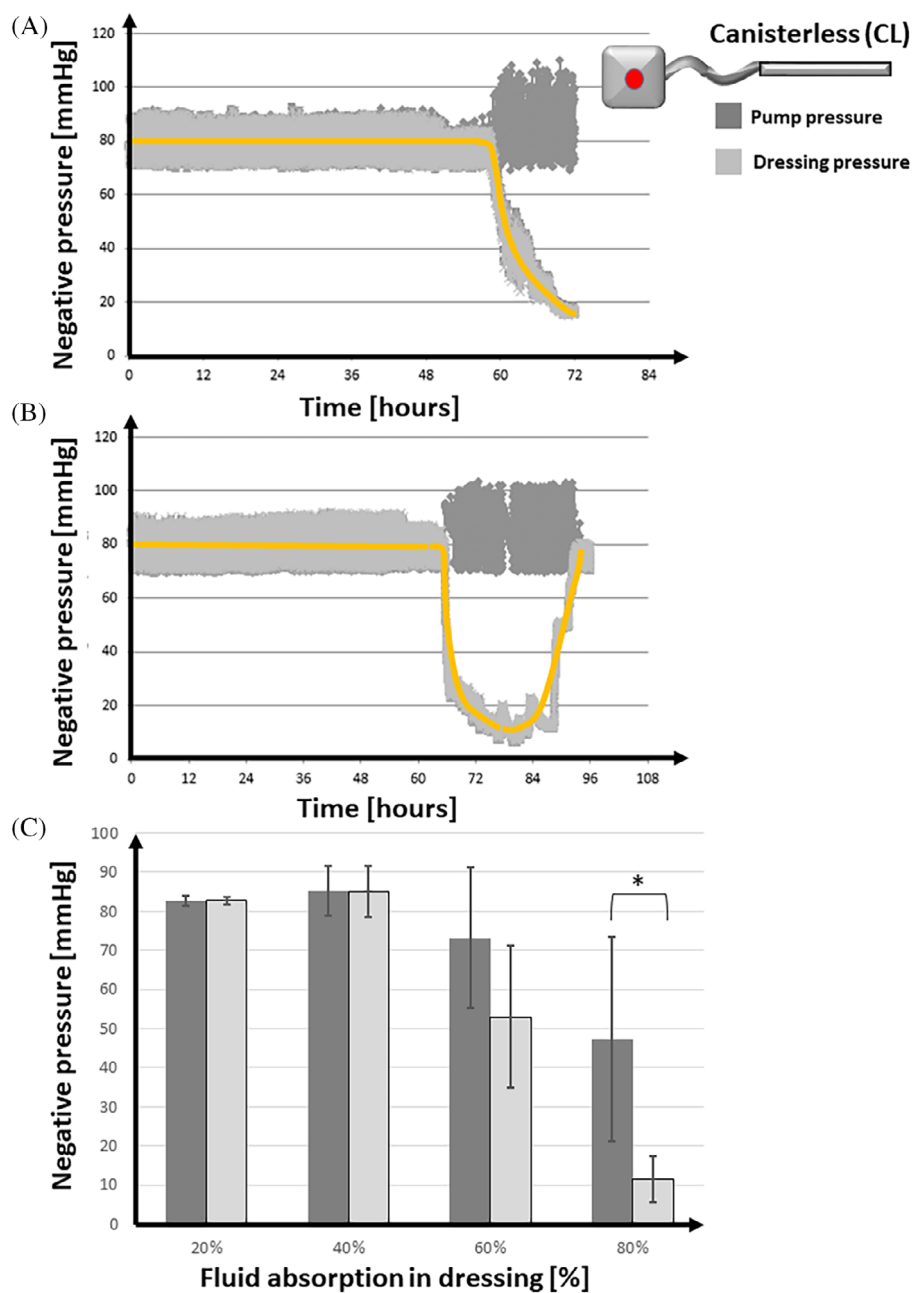


**FIGURE 2** Results from laboratory bench tests under conditions of simulated clinical use by application of the canisterless (CL) single-use negative-pressure wound therapy (suNPWT) system on a wound model simulating moderately and low exuding wounds for 72 and 96 hours, respectively. The negative-pressure output from the pump (dark grey) is plotted over time, vs the pressure level measured at the simulated wound bed under the absorptive dressing (light grey). Two common patterns were observed during this performance testing: (A) Delivery of negative pressure from the pump to the dressing is reduced over time, after approximately 2 to 3 days of simulated use, from a nominal level of  $-80$  mmHg to an absolute value lower than  $-20$  mmHg as fluid content builds up in the dressing of this CL suNPWT system. The flow rate of the simulated exudate has been set to simulate a moderately exuding wound, that is,  $1.1 \text{ g/cm}^2$  wound area/24-hours in this trial. (B) Delivery of negative-pressure from the pump to the dressing decreases from a nominal level of  $-80$  mmHg to an absolute value below  $-20$  mmHg, for a period of a day or more, until the fluid content in the dressing is reduced through evaporation to the environment, after which the delivery of negative pressure is eventually restored. In this trial, the flow rate of the simulated exudate has been set as low, that is,  $0.6 \text{ g/cm}^2$  wound area/24-hours. The orange lines are the trend lines of the pressure drops at the dressing, as a guide to the eye. (C) The means  $\pm$  SD of the negative pressures at the pump vs under the absorptive dressing when subjecting the CL suNPWT system to different levels of dressing saturations corresponding to application on a moderately exuding (flow rate =  $1.1 \text{ g/cm}^2$  wound area/24-hours) simulated wound for a duration of 72 hours ( $*P < .05$ ). Tests were repeated five times for each level of percentage-fluid absorption in the dressing



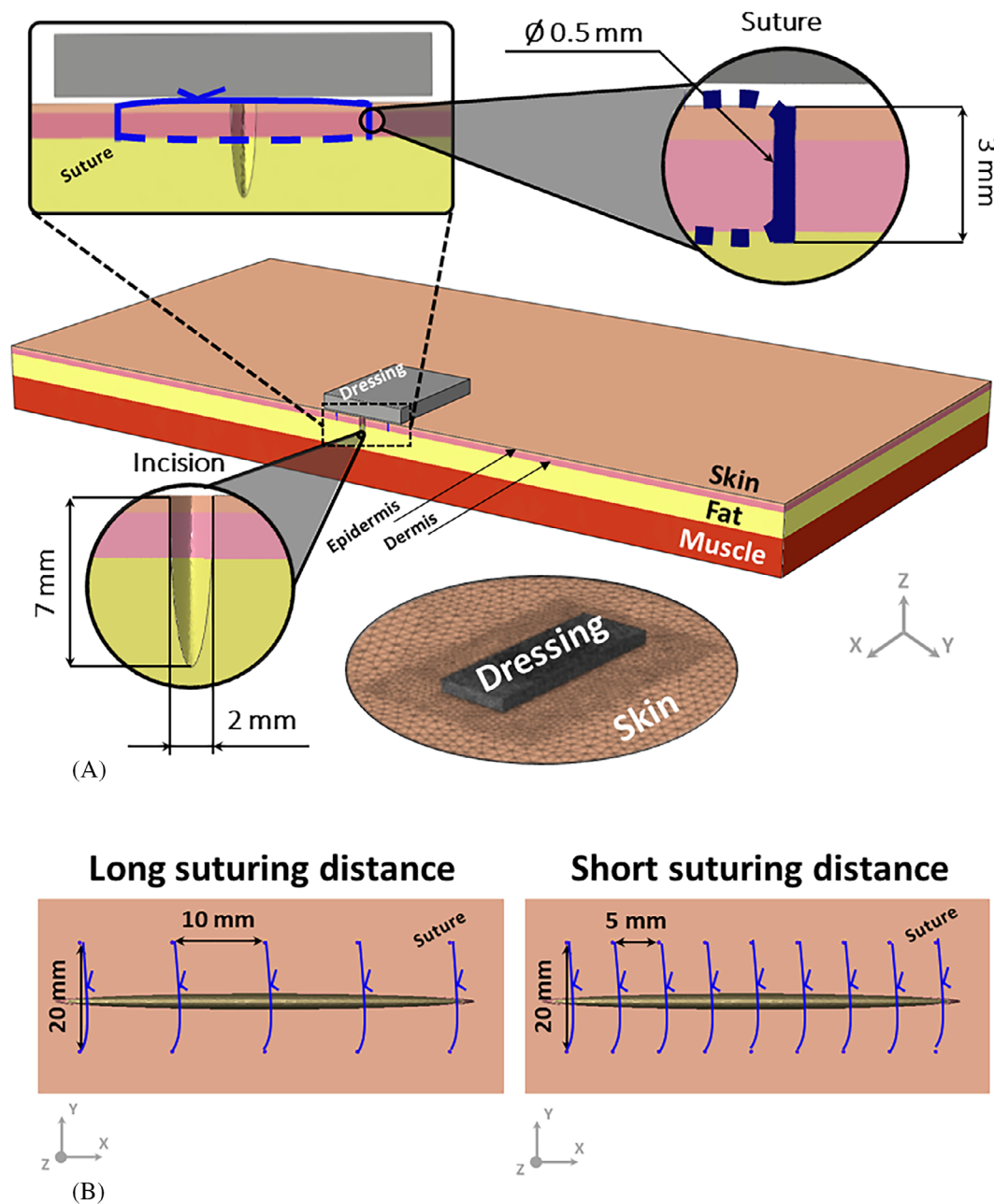


**FIGURE 3** Geometry and finite element modelling of the surgical incision model: (A) The model with its soft tissue components and the incision, which is closed using sutures and a single-use negative-pressure wound therapy (suNPWT) system, for which the dressing has been modelled here (the mesh of the dressing and skin in its vicinity is shown at the bottom frame; the mesh density has been increased towards the wound pad and incision region). (B) The two suture densities (high and low) used in the modelling

domain, whereas the superior (skin side) and inferior surfaces of the model were allowed to move in response to the applied negative pressures. The contacts between the different tissue layers (epidermis–dermis, dermis–adipose and adipose–muscle) were all set as ‘tie’ (‘no-slip condition’) (Figure 3A). Likewise, all sutures were set to have a ‘tie’ contact between their cylindrical surface and the surrounding soft tissues. The suture closure forces due to the tension suturing were simulated by displacing the

suture cylinders towards the wound (ie, along the Y-direction; Figure 3A) for mechanically closing the incision. Application of the dressing by a clinician on top of the sutured wound was simulated next, by displacing the entire dressing towards the skin above the incision site (ie, along the Z-direction), until full dressing–skin contact has been reached (Figure 3A; upper frame). Once this dressing–skin contact has been achieved, the suNPWT dressing was considered as being fully adhered to the

peri-wound skin, that is, no slippage was allowed between the dressing and skin (Figure 3A; bottom frame). Negative pressure was then simulated as hydrostatic compression, which was simultaneously applied to all the six surfaces of the dressing (the superior aspect, inferior aspect and the four sides). This resulted in a reduction in the dressing volume, from 12 to 8.7 cm<sup>3</sup> (28%) and 8.5 cm<sup>3</sup> (29%) for the CB and CL suNPWT systems, respectively.

### 2.2.3 | Protocol of computational simulations, numerical methods and outcome measures

The action of the suNPWT systems was simulated as static negative pressure, delivered through the applied dressing (Figure 3A). The CB system was considered to maintain a nominal negative pressure level of -125 mmHg throughout the entire period of use (hereunder 'CB-125'). For the CL system, however, while the nominal negative pressure level was set as -80 mmHg (hereunder 'CL-80'), we have also considered occasional pressure drops (as demonstrated to occur in the simulated clinical use experiments described above) due to the dressing approaching saturation (Figure 2). We specifically simulated pressure drops in the CL system that were at 20 mmHg intervals and which have reduced the negative pressure level below an absolute value of |-20| mmHg, based on our laboratory testing data (Figure 2). The aforementioned model geometry has been meshed using the Scan-IP module (R-2020.09) of the Simpleware software (Synopsys, Inc., Mountain View, California).<sup>29</sup> The meshing was performed semi-automatically, that is,

with manual refinements near the borders of the incision, each pair of the sutures and the dressing (Figure 3A). All the mesh elements were tetrahedral; the numbers of elements for each tissue type and the dressing are further listed in Table 2. All the FE analyses were conducted using the ABAQUS software suite (ver. 2020, Dassault Systems Simulia Corp., Johnston, Rhode Island). The model was analysed for the von Mises (effective) stresses in skin tissue (epidermis and dermis considered together) near the sutures, focusing on the mean stress concentrations that form around each suture (Figure 5). Accordingly, outcome measures for analysis of the stress concentrations around the sutures were the means of the von Mises stresses at 5-mm diameter cylindrical regions of interest that concentrically surrounded each suture throughout the entire skin depth. The mean stresses from each such tissue cylinder surrounding a suture were used to obtain the descriptive statistics of the peri-wound skin stress state around the sutures, for the LSD and SSD closure configurations and the applied CB vs CL suNPWT systems, as the skin heals and regains its stiffness postoperatively (Figures 6 and 7). Specifically, we had assumed that postoperatively, a fully repaired skin (and each of its layers) eventually recovers to 85% of the native skin stiffness (but does not return to the basal stiffness level), which is approximately the maximum amount of skin stiffness that can possibly be salvaged.<sup>19</sup> We therefore conducted our above stress calculations for incrementally increasing steps of skin stiffness, starting at approximately 25% of the native skin stiffness and ending at 85% of its native stiffness, which represents a post-operative healing process that under real-world conditions, may last from days to weeks (Figures 6 and 7). We further calculated the tensional suturing forces for

**TABLE 1** Results from the laboratory performance tests under conditions of simulated clinical use, demonstrating a difference in the fluid mass managed by the absorptive dressing and canister of a canister-based (CB), single-use negative-pressure wound therapy (suNPWT) system, vs the absorptive dressing of a canisterless (CL) suNPWT system over a test period of 72 hours

Dressing size [cm]	suNPWT system type	Total amount of fluid delivered to the dressing [g]	Amount of fluid retained in the dressing at the end of the test period [g]	Amount of fluid collected in the canister at the end of the test period [g]	Ratio of total amount of the fluid mass retained in the dressing over the total fluid mass managed by the suNPWT system [%]
10 × 20	CB	61.9	19.8 ± 0.9	28.32 ± 8.0	32
	CL		22.8 ± 0.76	N/A	37
25 × 25	CB	330	115.6 ± 6.1	73.9 ± 6.3	35
	CL		156.2 ± 14.4	N/A	47

*Note:* The dressings of the CL suNPWT system were consistently subjected to greater fluid content levels by the experimental wound model described in Section 2.1, simulating a moderately exuding (flow rate = 1.1 g/cm<sup>2</sup> wound area/24-hours) wound. Each test was repeated five times, and the amounts of fluid mass retained in the dressings are reported as means ± SD per test condition.

the CL and CB suNPWT systems, as well as the suture forces at baseline, where no suNPWT system is applied, separately for the LSD and SSD closure configurations.

### 2.3 | Wound healing study in a porcine model for closed incisions

The animal study described below was conducted under approval no. 01063.03 of the NAMSA Medical Device Testing Ethical Committee registered by the French Department of Agriculture (Chasse-sur-Rhône, France), to compare the wound healing performances of the CB-125 and CL-80 suNPWT systems.

The study included six female domestic pigs (Landrace-Large White cross), weighing 85 to 93 kg at the study start time. In each animal, three incision wounds with lengths of 6 cm and depths of 7 to 10 mm, extending to the deep fascia, were induced contralaterally on the back (Figure 8A). The cranial wounds (L1 and R1; Figure 8A) were in general mildly deeper than the caudal wounds (L3 and R3; Figure 8A), due to the anatomical site differences and constraints. The CB-125 and CL-80 suNPWT systems were applied to the three wounds on each side of the back in all the animals. All sites of application were randomised equally for the locations of the suNPWT systems of each type, that is, a suNPWT system of a certain type was placed on either the right (R1, R2, R3) or the left

back sides (L1, L2, L3), respectively (Figure 8A), so that the animal body side did not affect the acquired biomechanical data.

Nine wounds treated by each suNPWT system type (across the six animal group) were marked as sites for sampling of skin biopsies. These biopsies were taken using a biopsy punch (with diameter of 8 mm) and a scalpel, to reach the depth of the deep fascia (Figure 8C) at the days of NPWT dressing replacements, that is, on day 3 (from the cranial edge of the wound), day 6 (from the caudal wound edge) and day 10 post-injury (from the wound centre) (Figure 8B), thereby yielding a total of 27 biopsies per suNPWT system type. Biopsy sections were stained for histopathological and histomorphometric evaluations using modified Masson's Trichrome and Safranin-Haematoxylin-Eosin, to detect important wound healing characteristics, including infiltration of inflammatory cells (eg, lymphocytes and macrophages) to the vicinity of the wounds, as well as general necrosis, haemorrhage or other potential forms of tissue degeneration. At the study termination (day 14), all the animals were euthanised, and skin samples were collected and separated into two sets, one for performing the biomechanical tensile testing described below and the other, for histopathological and histomorphometric analyses as described above for the biopsies (Figure 8D).

For the biomechanical testing, a total of 30 porcine skin samples (12 of intact, uninjured skin and nine treated by each suNPWT system) were harvested from

TABLE 2 Mechanical properties of the model components

Model component	Coefficients		Viscoelastic material parameters				Numbers of elements	
	$C_{10}$	$D_1$	$g_1$	$\tau_1$ [s]	$g_2$	$\tau_2$ [s]		
Epidermis <sup>a,b,c</sup>	17.230 <sup>f</sup>	425	0.0864	0.212	0.214	4.68	67 012	
Dermis <sup>a,b,c</sup>	1.7230 <sup>f</sup>	4.25	0.0864	0.212	0.214	4.68	102 152	
Adipose <sup>a,b,c</sup>	0.001723	0.0425	0.3988	2.04	0.12381	76.96	133 037	
Muscle <sup>c</sup>	0.0355	0.34	4.836	0.016	0.423	8.59	16 977	
Dressing <sup>d</sup>	Dry	Canister-based	0.005	92.66	-	-	-	59 590
		Canisterless	0.003	155.84	-	-	-	
	Contains wound fluid	Canister-based	0.0025	184.61	-	-	-	
		Canisterless	0.0039	118.81	-	-	-	
$E$ [MPa]		$\nu$						
Sutures <sup>e</sup>	200 <sup>f</sup>	0.49	-	-	-	-	2453	

<sup>a</sup>Hendricks et al.<sup>30</sup>

<sup>b</sup>Xu and Lu.<sup>31</sup>

<sup>c</sup>Katzengold et al.<sup>21</sup>

<sup>d</sup>Measured in the present study.

<sup>e</sup>Greenwald et al.<sup>32</sup>

<sup>f</sup>We had assumed that postoperatively, a fully repaired skin (and each of its layers) eventually recovers to 85% of the native skin stiffness (but does not return to the basal stiffness level), which is approximately the maximum amount of stiffness that can possibly be salvaged.<sup>19</sup>



the animals immediately after the euthanasia and cut into dumbbell-shaped samples (with central width, thickness and length of  $12 \pm 1$ ,  $8 \pm 1$  and  $17 \pm 2$  mm, which were respectively oriented perpendicularly to the incision) (Figure 8D). The dumbbell skin samples were stored at  $-80^{\circ}\text{C}$  until the day prior to the measurements. A day before the measurements were performed, the samples were thawed overnight at  $4^{\circ}\text{C}$  while being submerged in fresh phosphate-buffered saline (PBS) solution. After thawing the skin samples, tensile tests to failure were conducted by means of a material testing machine (model Z010, ZwickRoell, Ulm, Germany), equipped with special tensile clamps for soft tissues (BOSE/TA Instruments, New Castle, Delaware) and a 500 N-load cell (accuracy  $\leq 0.24\%$ ). The dumbbell-shaped skin specimens were fixed within the clamps of the machine and tested at a deformation rate of 17 mm/min at ambient

conditions. Special care was taken to ensure proper axial alignment of each tissue specimen with respect to the tensile axis of the testing machine. Specimens were initially pre-conditioned for five loading cycles to a strain value of 10%, before loading them to their ultimate tensile strain (UTS), which has been defined here as the strain at the point of tissue failure. The maximum force recorded by the load cell of the testing machine at failure ( $F_{\text{max}}$ ) and the elongation at failure (in mm) were used to calculate the structural stiffness ( $k$ ) of each tissue specimen (in N/mm). Finally, an analysis of variance (ANOVA) was used to compare the values of  $F_{\text{max}}$ , UTS and the structural stiffness for the intact (uninjured) skin; the skin from wounds treated by means of the CB-125 suNPWT system; and the skin from wounds treated with the CL-80 suNPWT system, for a statistical significance level of  $P < .05$ .

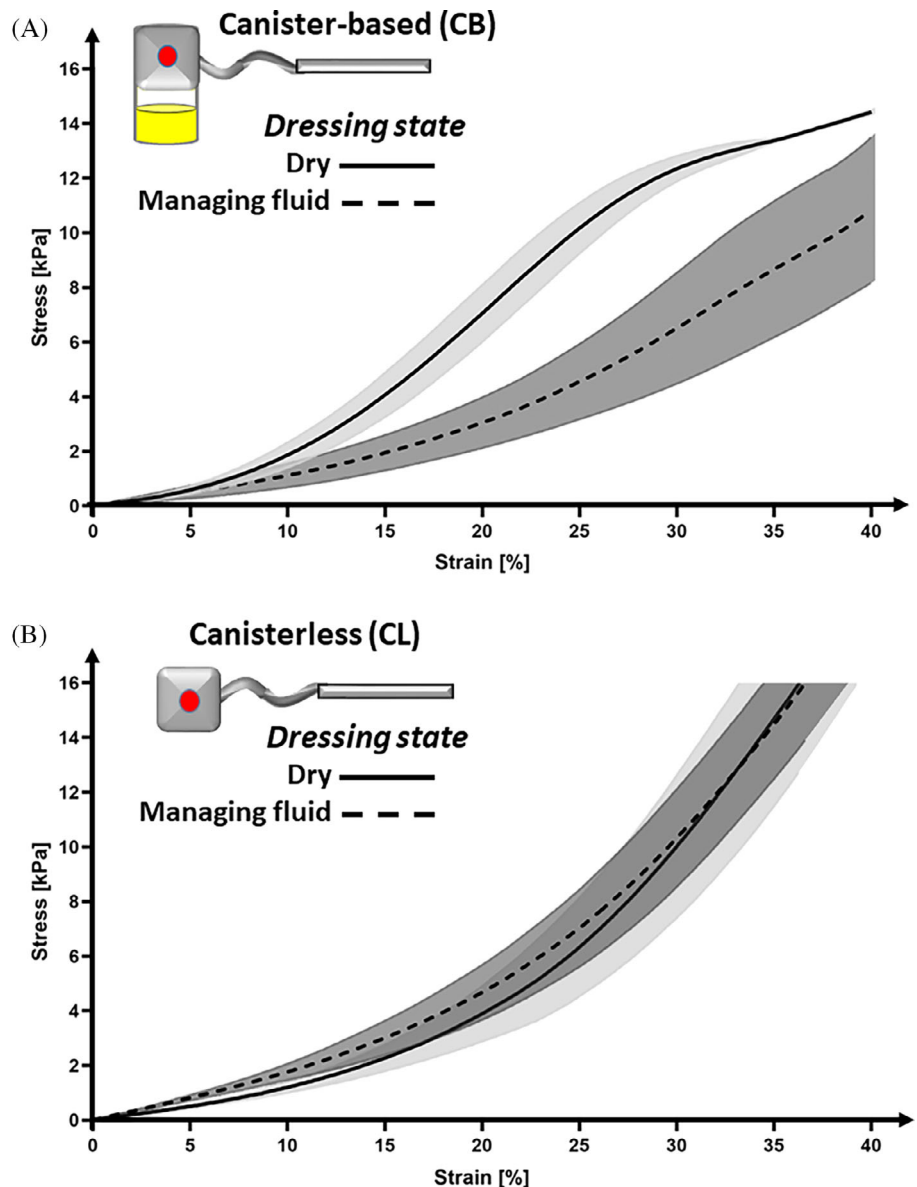


**FIGURE 4** Results of compression testing of dry vs dressings managing simulated wound fluid of: (A) the canister-based (CB) vs (B) the canisterless (CL) single-use negative-pressure wound therapy (suNPWT) systems. The dressings of the two suNPWT systems are shown to behave differently, where the dressing type of the CB suNPWT system softens after being submerged in a xanthan gum-based exudate-like fluid, as opposed to the dressing type of the CL system, which stiffens post the fluid-exposure. Each curve is the mean ( $\pm$ SD, shown as shaded areas) of 6 samples

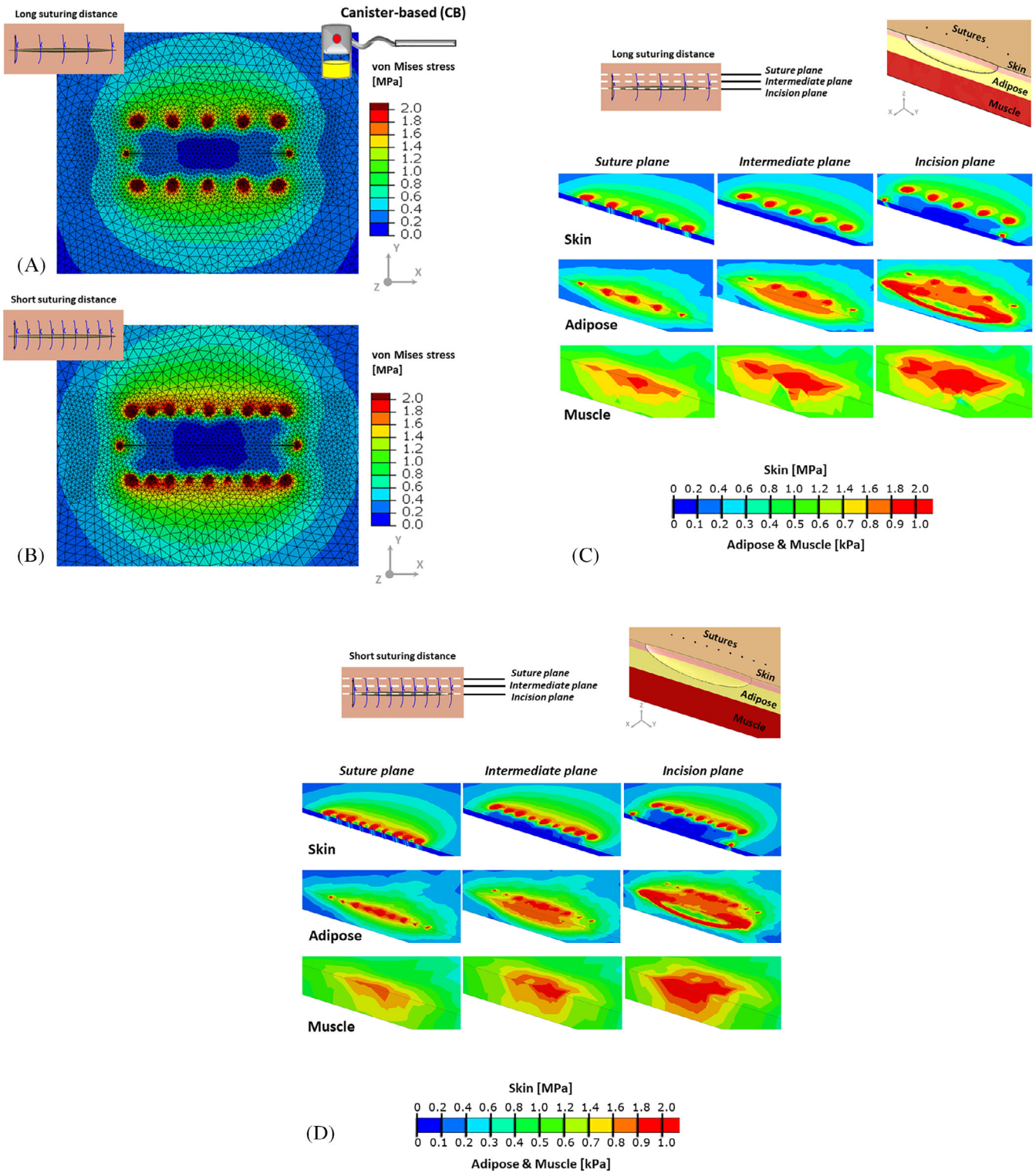
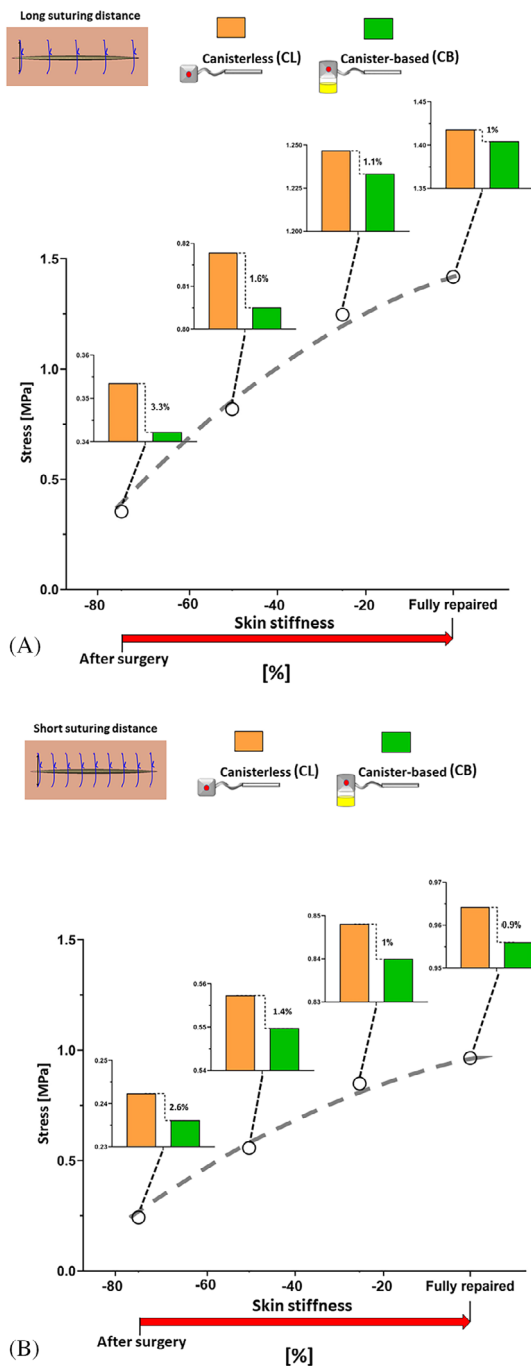


**FIGURE 5** Distributions of the von Mises (effective) stresses near the sutures, showing the stress concentrations around the sutures for the (A) long suturing distance (LSD) and (B) short suturing distance (SSD) model configurations from superior views and (C) for the LSD and (D) SSD configurations from three different cross-sectional views (the suture plane, the incision plane and an intermediate plane), for a steady negative-pressure level of  $-125$  mmHg. The dressing of the single-use negative-pressure wound therapy (suNPWT) system was hidden for the superior views (A, B) to reveal the stress concentration patterns on the peri-wound skin. Likewise, the tissue layers were separated for the cross-sectional views (C, D) to show the stress distributions at the skin–adipose and adipose–muscle interfaces

### 3 | RESULTS

#### 3.1 | Performance tests under conditions of simulated clinical use

For safe and effective therapy, it is required that the suNPWT system provides adequate fluid management, and in particular, it should continuously deliver the intended negative pressure to the wound, throughout the therapy period. Examples of negative pressure performance for the CL-80 suNPWT system are shown in Figure 2A,B.



Two common patterns of pressure delivery to the wound bed, with respect to the intended pressure levels at the pump, were observed during the simulated clinical use testing of this CL-80 suNPWT system: (a) Loss of the negative-pressure level delivered to the wound bed under the dressing over time, after approximately 2 to 3 days of use, from a nominal level of  $|-80|$  mmHg (delivered by the pump) to an absolute value below  $|-20|$  mmHg (measured under the dressing), as the dressing approached saturation (Figure 2A). (b) Loss of the negative-pressure level delivered to the wound bed, from a nominal level of  $|-80|$  mmHg to an absolute value lower than  $|-20|$  mmHg, for a period of a day or more, until the fluid content in the dressing was sufficiently reduced through evaporation to the environment, after which the delivery of the negative pressure produced by the CL system was restored (Figure 2B). Noteworthy is that when the CB-125 suNPWT system was subjected to the same test method and protocol of simulated clinical use, pressure drops between the pump and the simulated wound bed were not observed.

A more detailed analysis, evaluating the delivery of the intended negative-pressure level by the CL-80 suNPWT system when subjected to fluid management conditions corresponding to a 72-hours simulated application on a moderately exuding wound ( $1.1 \text{ g/cm}^2$  wound area/24-hours), revealed that the mean negative-pressure level in the dressing was statistically indistinguishable from that actually delivered by the pump only for the cases of the dressing managing up to 40% of the wound fluid simulant. However, for greater fluid contents in the dressing of the CL-80 suNPWT system, the negative pressures delivered to the simulated wound were substantially lower than the (nominal) intended negative pressure delivered from the pump (Figure 2C). Furthermore, the differences between the pressure delivered by the pump and the dressing pressure became statistically

**FIGURE 6** The mean von Mises (effective) stresses around the sutures after applying a canisterless (CL) vs a canister-based single-use negative-pressure wound therapy (suNPWT) system, for the (A) long (low-density) and (B) short (high-density) suturing distance model configurations, as the skin gradually heals and regains its stiffness postoperatively (which is represented as an increase in percentage stiffness with respect to the intact skin stiffness level). Of note, we assumed that postoperatively, a fully repaired skin (and each of its layers) eventually recovers to 85% of the native skin stiffness but does not return to the basal stiffness level. According to the literature, the 85% level is approximately the maximum amount of stiffness that can possibly be salvaged.<sup>33</sup> Possible occurrences of pressure drops during therapy by means of the CL suNPWT system are not considered for the simulation data shown here

significant for the high fluid levels in the dressing. For example, the CL-80 suNPWT system managing 80% of the expected fluid volume from a moderately exuding wound (for an anticipated dressing change once in

3 days), only delivered 24% of the pump pressure to the simulated wound ( $P < .05$  in a two-tailed, unpaired  $t$ -test; Figure 2C).

Further analyses of the fluid management performances of the dressings of the two suNPWT systems when subjected to simulated clinical use under the same test protocol, confirmed that a difference existed in the volumes of the fluids retained in the dressings of the CB-125 vs the CL-80 suNPWT systems over a test period of 72 hours. It was specifically observed that the dressings of the CL suNPWT system were consistently subjected to greater fluid contents during the simulated use tests (Table 1).

### 3.2 | Mechanical behaviour of the dressings

The results of the dressing compression tests (Figure 4) demonstrated a different behaviour for the two dressing types, where the dressing of the CB-125 suNPWT system softened when managing the exudate-like fluid (Figure 4A), in contrast to the dressing type of the CL-80

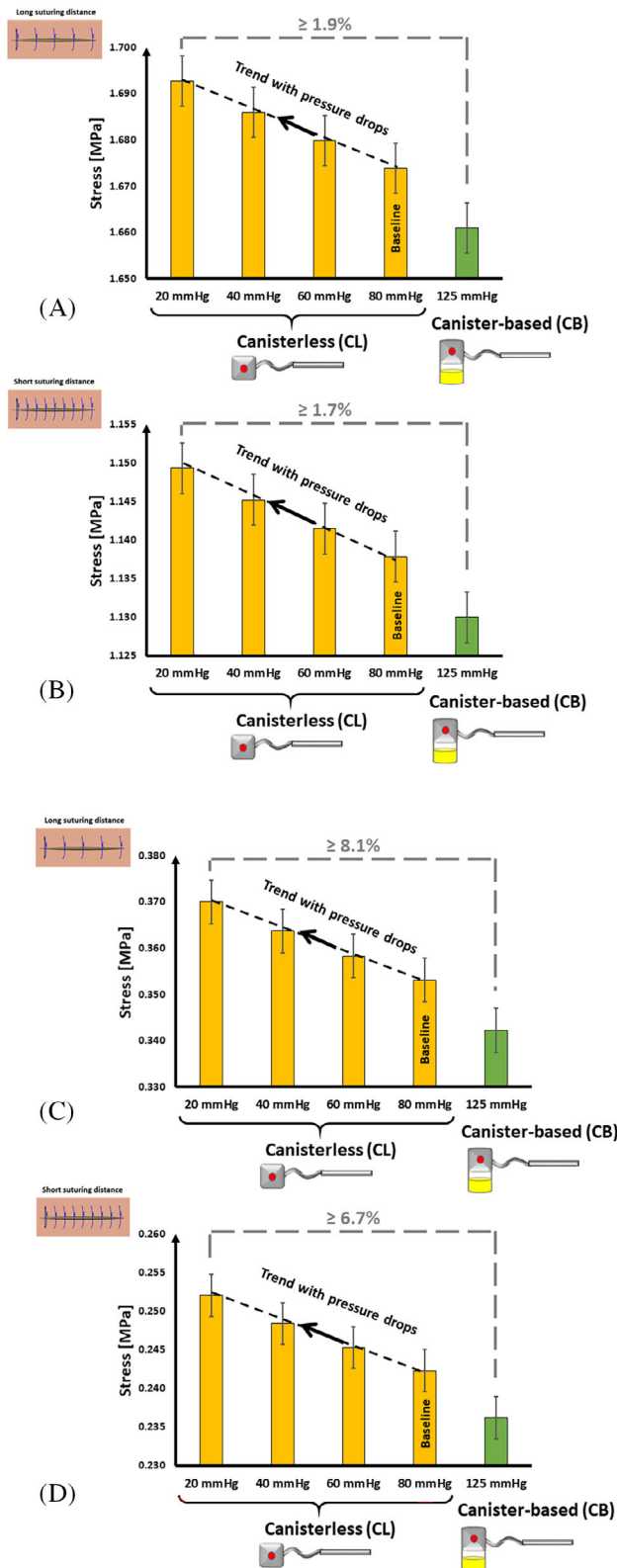
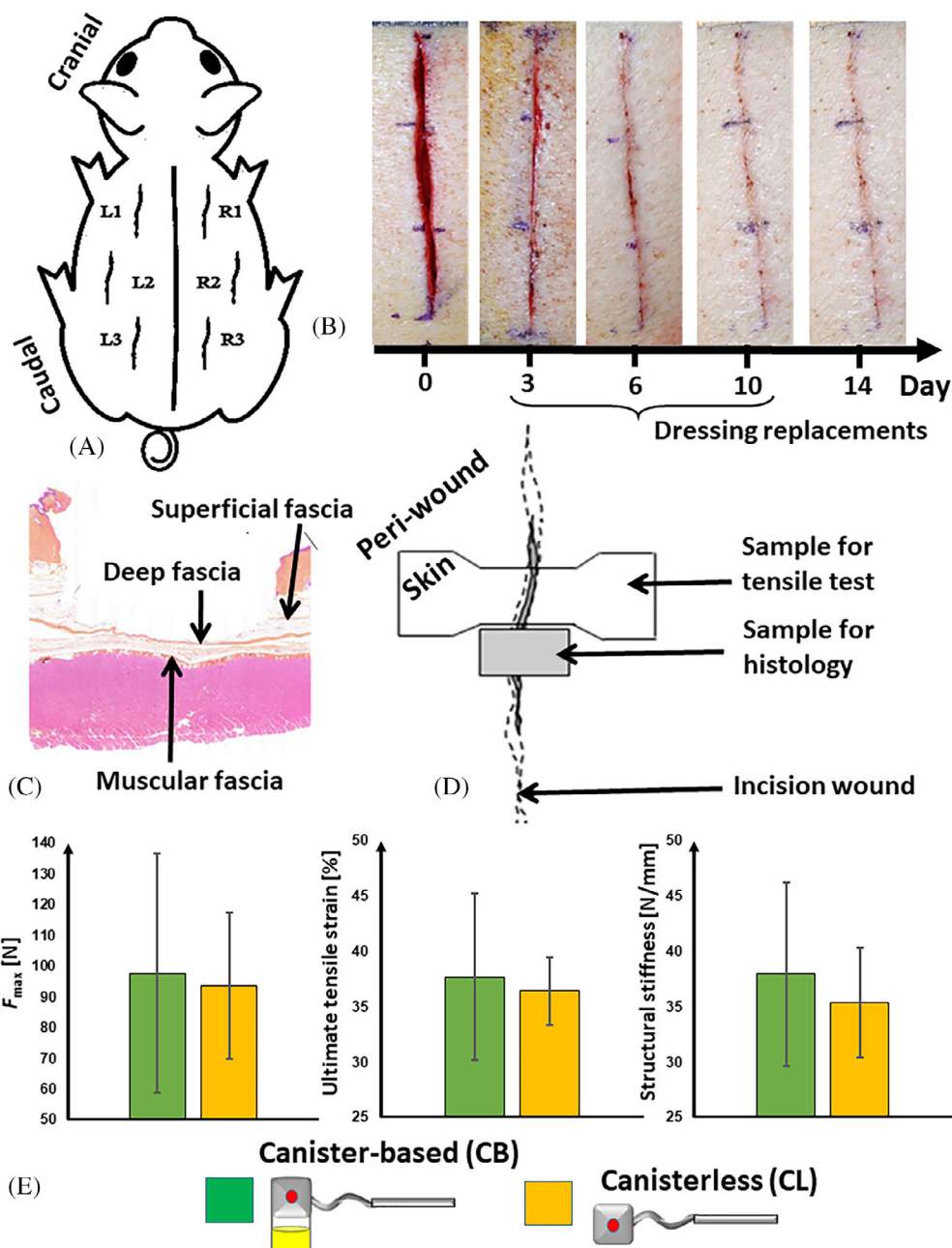


**FIGURE 7** The mean von Mises (effective) stresses around the sutures after applying the canisterless (CL) single-use negative-pressure wound therapy (suNPWT) system, for the (A, C) long (low-density) and (B, D) short (high-density) suturing distance model configurations. The simulation data in panels A and B consider the basal, intact (uninjured) skin stiffness, whereas the simulations in panels C and D consider a skin stiffness that is ~25% of the basal value, which is assumed to represent a compromised skin stiffness at the incision site near the time of surgery. All these simulations consider the potential occurrence of pressure drops for the CL suNPWT system when its dressing approaches saturation. Comparisons to the corresponding states of skin stresses that form when the canister-based (CB) suNPWT system is applied (green bars on the right hand side), and hence, the dressing remains far from saturation as excess fluid is constantly removed to the canister and are further included here. It is demonstrated that a drop in the negative pressure delivered by the CL suNPWT system implies that the tissue stress levels around the sutures increase proportionally with the decrease in the pressure output (the black dashed lines provide the guide to the eye for these tissue stress concentration trends). The tissue stress levels for the CB suNPWT system are lower than those for the CL system (for both suturing densities) already at baseline and prior to any potential pressure drop in the CL system, as the CB system operates on a greater (absolute) negative-pressure value. The stiffness changes of the dressings associated with the exposure to fluid, as reported here, have also been considered in these simulations. The error bars are the standard errors of the means



**FIGURE 8** The pre-clinical wound healing study in a closed incision porcine model evaluated the performance of the two single-use negative-pressure wound therapy (suNPWT) systems on the healing of incision wounds: (A) Locations of the 6 incision wounds on the animal back (L1, L2, L3 on the left side; R1, R2, R3 on the right side). (B) Example of a wound healing process for an incision treated with the canister-based (CB) suNPWT system over the course of the 14 study days. Dressings were changed at days 3, 6 and 10. (C) Histological image of a wound showing the depth of tissue damage that had been induced. (D) The location and orientation of skin specimens extracted for biomechanical tensile testing and histological analyses. (E) The means ( $\pm$ SD) of the biomechanical properties of skin treated by the CB vs the canisterless (CL) suNPWT systems, from left to right: Tensile force measured at skin failure ( $F_{\max}$ ), the ultimate tensile strain at failure and the structural skin stiffness



suNPWT system that mildly stiffened post the same fluid-exposure (Figure 4B).

### 3.3 | Computational study

Primary closure of the simulated surgical incisions by nylon sutures induced patterned stress concentrations in peri-wound skin around each suture, for both the LSD and SSD model variants (Figure 5). The sites of maximum peri-wound skin stresses within these stress concentration regions were located mostly in the sides opposite to the incision (Figure 5). Following simulated application of suNPWT near the time of surgery, where

the skin stiffness is still low (ie, 25% of the native skin stiffness), the peri-wound stress concentrations around the sutures for the CL-80 were approximately 3% greater than for the CB-125 system regardless of the suturing technique (Figure 6), given continuous delivery of the nominal negative pressure to the wound bed.

However, accounting for (a) the loss of performance for the CL suNPWT system following fluid management solely by the dressing, as demonstrated in the simulated clinical use tests which revealed considerable pressure drops from the nominal  $|-80|$  mmHg level (Figure 2) and (b) the stiffness rise for the dressing of the CL-80 system associated with fluid management, as reported here (Figure 4 and Table 2), the mean peri-wound skin



**TABLE 3** Percentage-change in average stresses around the sutures for the canisterless (CL) single-use negative-pressure wound therapy (suNPWT) system immediately after suturing and applying this CL suNPWT system and where pressure drops (absolute pressure <  $-80$  mmHg) occur

Pressure level	Long suturing distance		Short suturing distance	
	Stress reduction after suturing	Stress increase due to fluid buildup in the dressing	Stress reduction after suturing	Stress increase due to fluid buildup in the dressing
-20 mmHg	-0.4%	1.1%	-0.4%	0.9%
-40 mmHg	-0.8%	0.7%	-0.7%	0.6%
-60 mmHg	-1.2%	0.3%	-1.0%	0.2%
-80 mmHg	-1.5%	0.0%	-1.4%	0.0%

stresses for the CL suNPWT system were shown to rise proportionally to the extent of the pressure drop, irrespective of the suturing technique (Figure 7 and Table 3). The CB-125 suNPWT system does not suffer from compromised negative-pressure delivery (as excess fluid is transported to the canister), resulting in that the reduction of peri-wound skin stress levels for this system remains constant over time (Figure 7). When the skin had been repaired to the maximum possible extent, that is, to 85% of its native stiffness, the peri-wound skin stress concentrations around the sutures at each pressure drop episode of the CL suNPWT system may be up to approximately 2% greater with respect to the stress concentrations associated with use of the CB-125 suNPWT system (Figure 7A,B). Nonetheless, when the skin is relatively soft and vulnerable, near the time of surgery, the skin stress concentrations around the sutures associated with the CL suNPWT system can increase by up to approximately 7% to 8% at each pressure drop episode, with respect to the stress concentrations that apply when the CB-125 suNPWT system is used (Figure 7C,D). Noteworthy is that the peri-wound skin stress levels associated with the CB-125 suNPWT system were lower than those for the CL system for both suturing densities already at baseline conditions, that is, prior to any potential pressure drop in the CL system (Figure 7). The calculated forces on the sutures (Table 4) were consistent with the above skin stress data, further demonstrating that the suture forces associated with the use of the CL-80 system (functioning at its nominal  $-80$  mmHg pressure level) were 6%-greater than those that occurred for the CB-125 system, regardless of the suture density. Moreover, the CB-125 suNPWT system was able to reduce the mean suture forces by 13% and 8% for the LSD and SSD suture densities, respectively, with reference to the (no suNPWT) baseline (Table 4).

The above computational results (Figures 2 and 4) demonstrated differences in peri-wound skin stress exposures that are affected by: (a) The pressure level delivered

**TABLE 4** The calculated forces (mean  $\pm$  SD) on the sutures used for the primary closure in the computational modelling, depending on the negative-pressure level applied by the single-use negative-pressure wound therapy (suNPWT) system and the suture density

Negative-pressure level [mmHg]	Suture density	
	LSD [milli-Newton]	SSD [milli-Newton]
0 (no suNPWT system applied)	115 $\pm$ 56	87 $\pm$ 40
-80 (canisterless suNPWT system)	106 $\pm$ 53	85 $\pm$ 34
-125 (canister-based suNPWT system)	100 $\pm$ 52	80 $\pm$ 35

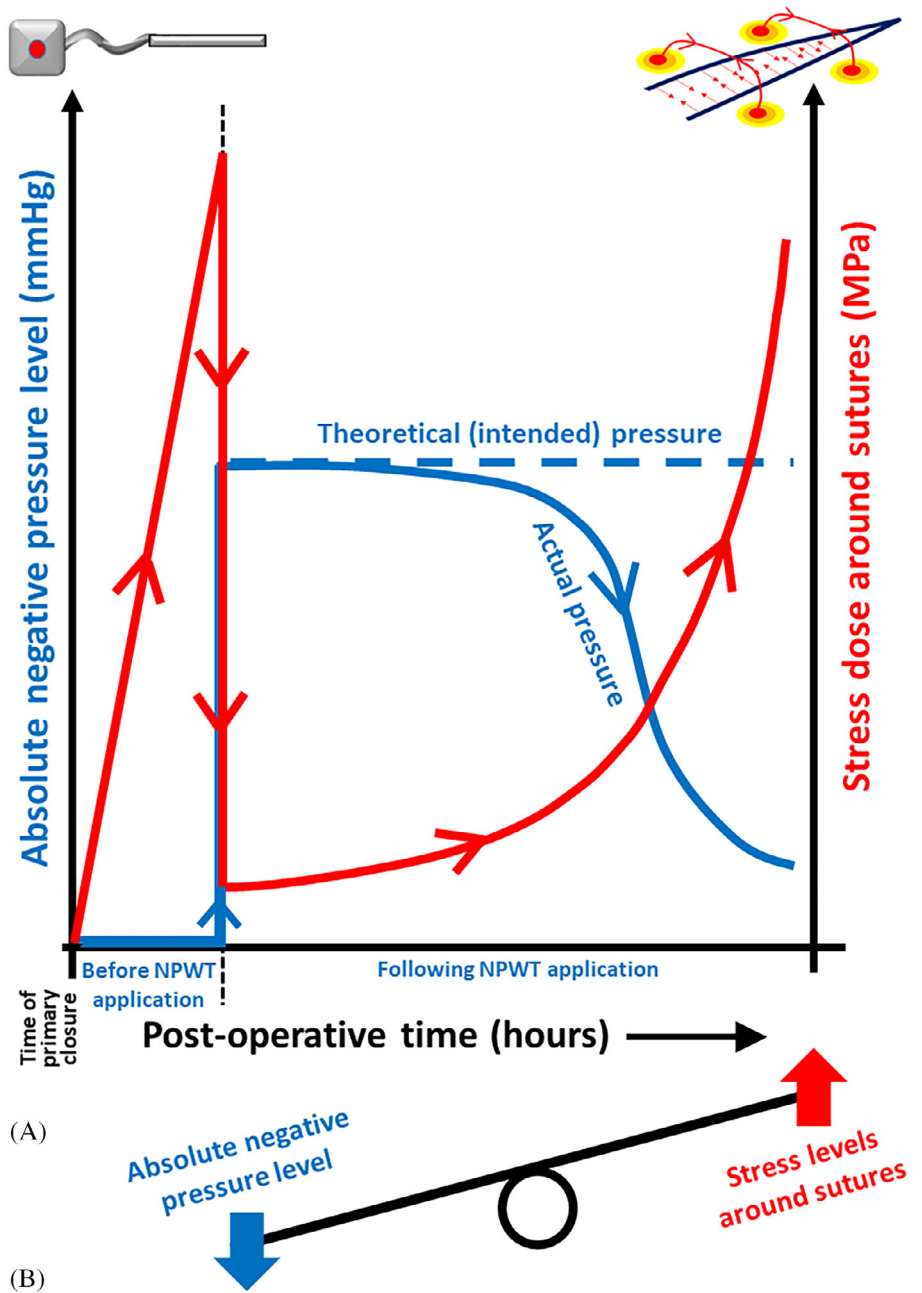
Abbreviations: LSD, long suturing distance; SSD = short suturing distance.

by the suNPWT system; (b) the technology for fluid management of the CL vs the CB system design, which has consequences on the stability of the delivery of continuous negative pressure and (c) the suturing technique used for the primary closure. In particular, the greater, continuous and steady negative-pressure level delivered by the CB-125 system provided the most effective reduction of skin stress concentrations around the sutures (Figures 5-7).

### 3.4 | Stress-dose calculations

The stress-dose outcome measure (Appendix A.2) quantifies the extent of the peri-wound skin exposure to a (potentially time-dependent) loading state over time. The stress-dose calculations, based on performance of the CL-80 vs the CB-125 suNPWT systems as detailed in Appendix A.2, demonstrated that a potential drift in the negative-pressure level of the CL system will gradually reduce the off-loading of tensile stresses around the

**FIGURE 9** Conceptualisation of the effect of the magnitude of the absolute negative-pressure level produced by the single-use negative-pressure wound therapy (suNPWT) system on the stress dose in peri-wound skin around the sutures: (A) The consequences of a pressure drop in a canisterless suNPWT system on the stress dose levels in peri-wound skin around the sutures, over a time course that ranges from the time of the primary suture closure, through the application of the NPWT system and later, when the system delivers pressures that are lower than the theoretical (expected) pressure level. (B) The swing between the absolute negative-pressure level and the peri-wound skin stress levels around the sutures. Once the absolute negative-pressure level drops, peri-wound skin stresses rise



sutures (Figure 1). Such pressure level drifts will therefore result in a rapidly climbing stress dose around the sutures, as the delivery of the (absolute value of the) negative-pressure level decreases (Figure 9A). Of note, in each of the aforementioned analytical examples (Equations [A4] and [A5]), the stress-dose difference (SDD) increases faster than the difference in the stress concentration level  $\Delta\sigma(t)$ ; also, the SDD increases faster for an exponential plateauing of the level of pressure (which was demonstrated experimentally in Figure 2A), with respect to the linear decay, since the difference in the stress concentration levels  $\Delta\sigma(t)$  increases sooner for the exponentially plateauing pressure case, relative to the linear drop pattern.

Without considering potential pressure drops for the CL-80 suNPWT system, the SDD between the two suNPWT system types is  $\Delta\sigma \times t$ , where  $\Delta\sigma$  is the difference between the skin stress concentration levels around the sutures for the two system types. In clinical settings, suNPWT is typically applied for multiple days following surgery, and hence, the  $\sim 3\%$  difference in skin stress levels which has been found here to be associated with the momentary nominal pressure difference between the CL-80 and CB-125 suNPWT systems (Figure 6) becomes considerable. For example, the aforementioned skin stress level difference translates to an SDD of  $\sim 70\%$ -hours (ie,  $\sim 3\% \times 24$  hours) over just the first day following application of the suNPWT system (at which time, the

contribution of biological healing to the mechanical load sharing is still minor<sup>19</sup>). Nevertheless, the latter SDD calculation is simple and does not consider any potential occurrences of pressure drops for the CL suNPWT system (such as those documented in the current laboratory work; Figure 2). A more realistic evaluation of the SDD should consider the occurrence of pressure drops for the CL suNPWT system, and, when these are considered, for either pressure drop pattern – of a linear or exponential nature – the abovementioned first approximation of an SDD of  $\sim 70\%$ -hours for a single treatment day becomes highly conservative. That is, any pressure drops for the CL suNPWT system, either recoverable or not (Figure 2), will increase the SDD considerably.

### 3.5 | Wound healing study in a porcine model

The results from the pre-clinical wound healing study overall demonstrated full wound closure, complete epithelialisation and mature tissue repair of all the studied incision wounds, without any adverse events. The biopsies extracted at the 3, 6 and 10-day time points demonstrated a normal wound healing cascade for both suNPWT system types, starting with fibroblast proliferation observed at day 3, then fibroplasia and collagen deposits at day 6 and a full inflammatory reaction at day 10. At the 14-day termination of the study, angiogenesis and formation of granulation tissue were evident through histology in all the animals and wounds, though the scarring process did not complete (Figure 8B). No maceration, erythema nor oedema was observed at the peri-wound skin, for wounds treated with either suNPWT system type.

With respect to the biomechanical outcome measures, the mean  $F_{\max}$ , UTS and stiffness values of the intact (uninjured) porcine skin were  $313.9 \pm 83.5$  N,  $105.3 \pm 22.7\%$  and  $43.5 \pm 15.1$  N/mm, respectively (mean  $\pm$  SD). It should be noted that 14 days post-injury are an early time point for assessing substantial tissue remodelling, and thus, the corresponding property values for the healed skin post-suNPWT treatments using both suNPWT system types (Figure 8E) adequately indicated that the repaired skin had considerably inferior strength properties compared to the intact, uninjured porcine skin. Accordingly, the  $F_{\max}$  and UTS of skin post-treatment were measured to be  $\sim 30\%$  and  $\sim 35\%$  of the basal  $F_{\max}$  and UTS levels, respectively, regardless of the suNPWT system (Figure 8E). The repaired skin stiffness measure was closer to the uninjured skin baseline and also varied more between the suNPWT system types, with the CB-125 suNPWT system achieving 87% of the intact,

healthy skin stiffness on average at the study termination (day 14), compared to only 81% for the CL-80 suNPWT system (Figure 8E), but without statistical significance.

Furthermore, while both suNPWT system types resulted in similar and complete epithelialisation and progress to healing of all wounds at the study termination, the histopathology analysis of the tissue samples from the study termination qualitatively demonstrated overall faster onset of epidermisation for the incision wounds treated with the CB-125 suNPWT system. This epidermisation included more epidermal differentiation and adherence to underlying granulation tissue, as indicated by the histopathological evaluation already at days 3 and 6 for the CB-125 suNPWT system but not until days 10 and 14 for the CL-80 suNPWT system. In accordance with this observation, the mean  $F_{\max}$ , UTS and stiffness values of the porcine skin were mildly but consistently greater for the CB-125 suNPWT system with respect to those obtained for the CL-80 suNPWT system (Figure 8E). Specifically, the biomechanical property ratios for the  $F_{\max}$ , UTS and  $k$  values associated with the CB-125 over those of the CL-80 suNPWT systems were 1.043, 1.037 and 1.072, respectively, that is, all were greater than unity, although the relevant ANOVA testing indicated no statistical significance.

## 4 | DISCUSSION

Among the advanced wound care approaches, NPWT is presently considered a first line treatment for managing a variety of serious wound types,<sup>6-8,34-36</sup> very likely due to its relative ease of use and removal and low risk of complications.<sup>37</sup> In the last decade, NPWT has also been widely adopted for the management of surgical incisions.<sup>33,38</sup> For closed incisions, post-surgical complications such as infections or dehiscence can prolong the length of hospital stays, thereby imposing additional direct and indirect costs.<sup>39,40</sup> Single-use, CB or CL NPWT systems are a relatively new wound care technology, which is well suited for post-surgical care, to improve the rate of healing of incision wounds and reduce the occurrence of the aforementioned complications.<sup>13,41,42</sup> Treatment by means of suNPWT systems is gradually replacing the more traditional method of wound care through stationary NPWT devices.<sup>9,12,43</sup> The present work was aimed to evaluate the performance of a CL vs a CB suNPWT system, each with a different intended negative-pressure magnitude and technologies for fluid management. For this purpose, we developed a computational FE modelling framework, a laboratory bench-test for simulated clinical use and had further conducted a pre-clinical wound healing study in a porcine model for

closed incision. We specifically focussed on the importance and impact of effective fluid management for continuous delivery of the intended negative pressure by the suNPWT system and the impact of potential loss of the negative-pressure level over the period of therapy. Continuous delivery of the specified and intended level of negative pressure to the wound bed by the applied suNPWT system is hypothesised here to be important for promoting the wound healing. Specifically, a stable negative pressure moves and maintains the wound edges closer together and, thus, contributes to relief of the suture forces (Table 4). This in turn leads to a reduction of the stress concentrations in skin around the sutures (Figure 1), which enhances the nutritive perfusion and, hence, improves the wound healing.

Primary closure of a surgical incision using sutures involves a risk for post-surgical complications which range from seromas, hematomas and persistent swelling to skin and adipose necrosis (which promotes infections) in the short-term, to formation of hypertrophic or keloid scars in the long-term.<sup>18,19</sup> In this regard, updated systematic reviews and meta-analyses demonstrated association between the use of NPWT and reduction in serohaematoma formations and surgical site infections, indicating that generally, NPWT contributes to a lower occurrence of postsurgical peri-wound skin breakdown.<sup>44-48</sup> Localised elevated skin stresses resulting in ischaemia around the focal tension points caused by the sutures (Figures 1 and 5) are a critical factor contributing to the above complications.<sup>20</sup> The computational results presented here indicated that a continuous delivery of negative pressure at  $-125$  mmHg is advantageous with respect to the lower pressure level used in some commercial suNPWT systems ( $-80$  mmHg), in reducing the stress concentration levels around sutures (regardless of the suturing technique) (Figures 1 and 6). This is consistent with our published work which demonstrated that the pressure level set in the NPWT system has considerable influence on the peri-wound loading state, particularly with regards to peri-wound skin.<sup>20-22</sup> Moreover, a CL suNPWT system may suffer from loss of therapy effectiveness, as its dressing approaches saturation when excess exudate is not transported away from the dressing (as documented in Figure 2), thereby impeding delivery of the intended negative pressure.

Loss of therapy effectiveness by drops of the negative pressure further causes less reduction of the lateral tension in the wound (Figure 1), and, thereby, the skin stress concentrations around the sutures intensify (again, irrespective of the primary closure technique; Figure 7C, D), which theoretically increases the risk for skin ischaemia and the aforementioned postoperative complications.<sup>20</sup> Consistent with this theory, an animal study

conducted here to compare the performances of the two suNPWT system types under investigation, indicated a mildly better (though not statistically significant) repaired tissue quality for the surgical wounds treated using the CB-125 suNPWT system (Figure 8E). The results from the present animal study specifically showed that the mean maximum force to skin failure, the UTS and the structural stiffness were all mildly greater for skin at and near the incisions treated by means of the CB-125 suNPWT system (Figure 8E). Of note, Chen and colleagues<sup>49</sup> recently used shear wave elastography to demonstrate that in a rabbit model, the stiffness of wounded skin increases during NPWT-supported healing; however, the rise in the stiffness of the repaired skin depends on the NPWT protocol, and, specifically, on the level of the delivered negative pressure. The extent of skin stiffness changes in their work appeared to be more sensitive to the magnitude of the delivered negative pressure nearer the time of infliction of the surgical wound; after 1 day, negative pressure levels of  $-125$  or  $-150$  mmHg led to mildly greater elastic moduli of the wounded skin than negative pressures of  $-50$  or  $-80$  mmHg.<sup>49</sup> The results of the animal study presented here (Figure 8E) confirm these findings reported by Chen and colleagues<sup>49</sup> and can be attributed to the difference in the reduction in stress doses around the sutures induced by each suNPWT system type, as the stress dose describes the exposure of tissues to the varying stress state throughout the healing period,<sup>50</sup> and, thereby, is very likely to have an impact on the healing process and outcomes.

With the above being said, it should be clarified that there is no mechanobiological justification for arbitrarily and excessively increasing the absolute negative pressure-magnitude in an attempt to suppress the tension in the sutures. There is likely a 'sweet spot' of an absolute pressure level for each individual patient, above which increasing the pressure would counteract the positive effects described above, by compromising the localised blood circulation. Adequate perfusion is required to supply the cellular and metabolic demands for progressing through the wound healing phases. Poor perfusion is associated with wound complications including dehiscence, infections and delayed healing. Consensus work among a panel of NPWT experts reported that safe and effective therapy should be in the range of  $-50$  to  $-150$  mmHg; greater absolute pressure levels either showed no further benefit or were associated with a detrimental effect.<sup>51</sup> Borgquist and colleagues further stated that therapy at the lower pressure range (ie, at around or less than  $|-50|$  mmHg) is considered safe, however, may be clinically ineffective in terms of the exudate management and contribution to therapy.<sup>52</sup> At the high absolute



pressure domain (approximately  $|-150|$  mmHg and above), the NPWT may be painful and, if applied on poorly perfused wounds (eg, diabetic foot ulcers or thin skin transplants), may exacerbate the ischaemia at the wound edges.<sup>53,54</sup> High absolute pressure magnitudes are therefore generally not recommended or, under special circumstances, should be used with caution in patients with compromised vascularity.<sup>53,54</sup> Accordingly, increasing the NPWT absolute pressure levels beyond  $|-150|$  mmHg is not a valid approach for relief of the suture forces and the associated skin stresses.

For a CL suNPWT system, where there is no continuous clearance of the exudate from the absorptive dressing, compromised fluid management due to a saturated dressing may negatively impact the ability of the pump to deliver its intended negative pressure continuously to the wound during therapy (Figure 2). The theory of how a dressing of a CL suNPWT system which approaches saturation may compromise therapy performances due to loss of the applied negative pressure is depicted in Figure 9A. After closing a surgical incision, the clinical team has to make a decision regarding the type of the NPWT system that should be applied postoperatively, that is, stationary or single-use and if the latter, whether to apply a CB or a CL suNPWT system. The current evidence-based trend, particularly in orthopaedic surgery, to mobilise patients as soon as possible after they have had their surgical procedure contributes to the growing preference of suNPWT system, which facilitates such patient mobility. However, the specific choice of a suNPWT system has potential impact on the healing rate and the quality of the repaired tissues, as suNPWT systems may also differ substantially in technology, as highlighted in this work. This study provides both experimental and computational indications that a suNPWT system delivering a relatively greater negative pressure and applying controlled fluid management (ie, enabling the system to maintain the negative pressure by transporting excess fluid to the canister), is more likely to achieve better clinical outcomes. In particular, this work demonstrated that the occurrence of loss of the intended negative pressure diminishes the reduction of stresses around the sutures, resulting in an increase of the skin stress levels around the sutures (Figure 9B).

Validation of the computational results reported here was possible with respect to experimentally reported tensional suture forces. Specifically, Lear and colleagues measured suture forces in incisions of 11 male and 7 female patients aged 46 to 91 years, who presented for removal of skin cancers, following which the incision was closed by three sutures.<sup>55</sup> Using a commercial, calibrated force gauge, they measured a mean force of 0.52 N on the (individual) last suture, which translates to

approximately  $0.52/3 = 0.17$  N per suture. They did not apply NPWT to the incisional wounds in their study.<sup>55</sup> Our calculated baseline suture force levels (for the no suNPWT simulations) were 0.12 N and 0.09 N for the LSD and SSD suture densities, respectively, which resembles the empirical force levels reported in the Lear study. The minor differences can be explained by the fact that the mean force level in the sutures decreases non-linearly with each added suture<sup>55</sup>; however, Lear et al used only three sutures for closing the wounds they had treated. Related to this latter point, we demonstrated here that the difference between the performance of the CB and CL suNPWT systems in reducing the skin suture stresses increases for the LSD (ie, for a lower number of sutures) with respect to the SSD, as shown in Figure 6. For example, immediately post surgery, the CB-vs-CL skin stress difference for the LSD closure was 3.3% (Figure 6A), with respect to 2.6% for the SSD closure (Figure 6B).

Kazmer and colleagues had calculated that a standard, United States Pharmacopeia (USP) #4 suture having a diameter of 0.2 mm would generate compressive stresses in the order of 4000 mmHg to provide 0.1 N of closure force to 1 mm thick skin ( $0.1/0.2 \times 1 = 0.5$  MPa<sup>56</sup>). Of note, they did not include the shear stresses in skin in their aforementioned stress evaluation.<sup>56</sup> Their above calculations are in precise agreement with our current tensional closure force results (Table 4; no suNPWT system) and in further agreement with our post-surgical skin stress calculations (Figure 6). The skin perfusion pressure (SPP) in intact, uninjured skin is approximately 50 to 100 mmHg.<sup>57</sup> This normative SPP range is 80 times to 40 times less than the localised compressive stresses induced by sutures directly at their insertion sites, implying that the insertion sites of sutures are, by definition, ischaemic (with or without the contribution of a suNPWT). Naturally, skin perfusion occurs primarily between the sutures, away from the sutures (towards the wound edges) and through subcutaneous tissues below the skin. However, the sooner that the suturing forces are not required to maintain the edges of the wound tightly together (as that role is gradually taken by bridges of collagenous, scar tissue which gradually contract), the better the skin perfusion becomes. This underpins the role of a suNPWT system in continuously participating in the lateral tension and, in particular, in contributing to a more uniform closure pattern, as opposed to sutures which function discretely to achieve that goal. Noteworthy however, is that the localised tissue stresses desired and imposed near the closed wound site, with or without a suNPWT system, will vary with the patient, their skin thickness and skin health status, the anatomical location, and the suturing technique (as also demonstrated here<sup>56</sup>). This prevents the determination of



a certain generic and ultimate threshold for the desired extent of participation of the suNPWT system in the loading; however, sufficient and consistent therapy are key factors for clinical success.

A suNPWT system biomechanically interacts with the suturing technique, as a larger number of sutures would result in less force on each suture, thereby facilitating a greater potential contribution of the suNPWT system to a relief of the skin stress concentrations around the sutures (Table 4). We therefore conducted a dual analysis of the FE modelling outcome measures throughout, for two suturing techniques, LSD and SSD, as a sensitivity analysis. Whilst clinicians are unlikely to alter their suturing technique (but rather, will be choosing between suNPWT system types for the post-surgical care), we demonstrated here that the density of the sutures used in the clinical practice does not alter the main conclusions from this work.

As with any study, limitations exist and should be acknowledged. Firstly, in the computational modelling work, we assumed uniform thicknesses of the tissue layers and isotropic stiffness properties, whereas in reality, tissue thicknesses vary and directional preference of stiffness may exist, particularly for skin and muscle and depending on the specific anatomical site. However, our aim here was to represent a generic simulated anatomical configuration and incision wound, rather than limiting the scope to a specific anatomical site or surgical procedure. Modelling a generic anatomical configuration allowed to focus on the effects of the type of the suNPWT system on the skin stress levels around the sutures, which was the primary purpose of this work. With that said, it should be noted that non-uniformities in tissue thicknesses or stiffnesses, body curvatures or skin folds and irregular anatomical features at or near the incision site may contribute to the intensities of the formed tissue stress concentrations and amplify the trends of effects identified here (Figure 7). In a bioengineering research framework, however, this would have caused the computational results to be more difficult to interpret, which justifies the uniform tissue thicknesses and choice of the incision shape made here for the specific study objectives. The simulated clinical use performance tests were designed to mimic the real-world clinical practice; however, evaporation of wound exudates would depend on a variety of factors not considered in a laboratory setting, such as random changes in the ambient (temperature and humidity) conditions, or the core body temperature cycle related to the individual circadian rhythm. Another potential limitation is the relatively small number of animals that were tested, which perhaps lowered the statistical power; however, animal studies in acute wound care trials are restricted for ethical reasons and accordingly,

sensible compromises related to the number of animals assigned to this study were made in this regard when designing the research work, to optimise the above considerations. Lastly, for the computational modelling work, some of the tissue mechanical properties, particularly the viscoelastic coefficients of stiffness and relaxation times for adipose and muscle (Table 2), have been adopted from our published animal studies.<sup>58,59</sup> These tissue mechanical properties were used for the present simulations because accurate relaxation coefficients (ie, for a near-step response to a deformation load) are unavailable for fresh human adipose and muscle tissues but had been acquired from fresh animal tissue specimens in the aforementioned works.

In this work, we aimed at representing the mainstream of the surgical patients prescribed with suNPWT; however, future research steps may include studies of suNPWT treatments in patients with specific conditions that impose a greater risk for surgical complications, such as patients with tendency for developing a severe oedematous response, patients with type-2 diabetes and those suffering from obesity. Representing these subpopulations of surgical patients would require changes in the modelling framework to represent altered soft tissue stiffness behaviours, or abnormal tissue composition or both.

In closure, portable suNPWT systems are generally an elegant concept for post-surgical wound care; however, for a suNPWT system to facilitate the full benefits of the prescribed therapy, it should provide effective fluid management and continuous delivery of the intended (nominal) negative pressure magnitude to the wound. We conclude that a suNPWT system providing a greater (absolute) negative-pressure magnitude, and which delivers its intended negative pressure through controlled fluid management technology by removing the excess fluid from the dressing throughout the time course of the prescribed therapy, is advantageous from a bioengineering performance perspective. A sufficiently high and importantly stable delivery of the negative pressure via the dressing to the incision wound is more likely to facilitate better clinical outcomes, particularly concerning the biomechanical quality of the repaired tissues.

## ACKNOWLEDGEMENTS

This project has received funding from the European Union's Horizon 2020 research and innovation programme under the Marie Skłodowska-Curie Grant Agreement No. 811965; project STINTS (Skin Tissue Integrity under Shear). This work was also partially supported by the Israeli Ministry of Science & Technology (Medical Devices Program Grant no. 3-17421, awarded to Professor Amit Gefen in 2020) and by Mölnlycke Health Care (Gothenburg,

Sweden) for which Professor Gefen is a member of the Global Pressure Ulcer/Injury Advisory Board.

## ENDNOTE

\* Horse serum matches the viscosity, osmolarity and pH levels of wound fluids typically seen in patients.

## DATA AVAILABILITY STATEMENT

The data that support the findings of this study are available from the corresponding author upon reasonable request.

## ORCID

Amit Gefen  <https://orcid.org/0000-0002-0223-7218>

## REFERENCES

- Morykwas MJ, Argenta LC, Shelton-Brown EI, McGuirt W. Vacuum-assisted closure: a new method for wound control and treatment: animal studies and basic foundation. *Ann Plast Surg.* 1997;38(6):553-562. doi:10.1097/0000637-199706000-00001
- McLean WC. The role of closed wound negative pressure suction in radical surgical procedures of the head and neck. *Laryngoscope.* 1964;74(1):70-94. doi:10.1002/lary.5540740106
- Saxena V, Hwang CW, Huang S, Eichbaum Q, Ingber D, Orgill DP. Vacuum-assisted closure: microdeformations of wounds and cell proliferation. *Plast Reconstr Surg.* 2004;114(5):1086-1096. doi:10.1097/01.PRS.0000135330.51408.97
- Argenta LC, Morykwas MJ. Vacuum-assisted closure: a new method for wound control and treatment: clinical experience. *Ann Plast Surg.* 1997;38(6):563-577. doi:10.1097/0000637-199706000-00002
- Borgquist O, Gustafsson L, Ingemansson R, Malmjö M. Micro- and macromechanical effects on the wound bed of negative pressure wound therapy using gauze and foam. *Ann Plast Surg.* 2010;64(6):789-793. doi:10.1097/SAP.0b013e3181ba578a
- Bollero D, Carnino R, Risso D, Gangemi EN, Stella M. Acute complex traumas of the lower limbs: a modern reconstructive approach with negative pressure therapy. *Wound Repair Regen.* 2007;15(4):589-594. doi:10.1111/j.1524-475X.2007.00267.x
- Kamolz LP, Andel H, Haslik W, Winter W, Meissl G, Frey M. Use of subatmospheric pressure therapy to prevent burn wound progression in human: first experiences. *Burns.* 2004;30(3):253-258. doi:10.1016/j.burns.2003.12.003
- Armstrong DG, Lavery LA. Negative pressure wound therapy after partial diabetic foot amputation: a multicentre, randomised controlled trial. *Lancet.* 2005;366(9498):1704-1710. doi:10.1016/S0140-6736(05)67695-7
- Banasiewicz T, Banks B, Karsenti A, Sancho J, Sekác J, Walczak D. Traditional and single use NPWT: when to use and how to decide on the appropriate use? Recommendations of an expert panel. *J Chem Inf Model.* 2019;53(9):21-25.
- Delhougne G, Hogan C, Tarka K, Nair S. A retrospective, cost-minimization analysis of disposable and traditional negative pressure wound therapy Medicare paid claims. *Ostomy Wound Manage.* 2018;64(1):26-33.
- Apelqvist J, Willy C, Fagerdahl AM, et al. EWMA document: negative pressure wound therapy: overview, challenges and perspectives. *J Wound Care.* 2017;26:S1-S154. doi:10.12968/jowc.2017.26.Sup3.S1
- Brandon T. Using a single-use, disposable negative pressure wound therapy system in the management of small wounds. *Wounds UK.* 2016;EWMA SPECIAL:70-73.
- Brandon T. A portable, disposable system for negative-pressure wound therapy. *Br J Nurs.* 2015;24(2):98-106. doi:10.12968/bjon.2015.24.2.98
- Tettelbach W, Arnold J, Aviles A, et al. Use of mechanically powered disposable negative pressure wound therapy: recommendations and reimbursement update. *Wounds.* 2019;31(2 Suppl):S1-S17.
- Willy C, Agarwal A, Andersen CA, et al. Closed incision negative pressure therapy: international multidisciplinary consensus recommendations. *Int Wound J.* 2017;14(2):385-398. doi:10.1111/iwj.12612
- Karlakki S, Brem M, Giannini S, Khanduja V, Stannard J, Martin R. Negative pressure wound therapy for management of the surgical incision in orthopaedic surgery. *Bone Joint Res.* 2013;2(12):276-284. doi:10.1302/2046-3758.212.2000190
- Hudson DA, Adams KG, Van Huyssteen A, Martin R, Huddleston EM. Simplified negative pressure wound therapy: clinical evaluation of an ultraportable, no-canister system. *Int Wound J.* 2015;12(2):195-201. doi:10.1111/iwj.12080
- Ritchie SA. Skin surgery: prevention and treatment of complications - UpToDate. <https://www.uptodate.com/contents/skin-surgery-prevention-and-treatment-of-complications>. Accessed February 9, 2021.
- Commander SJ, Chamata E, Cox J, Dickey RM, Lee EI. Update on postsurgical scar management. *Semin Plast Surg.* 2016;30(3):122-128. doi:10.1055/s-0036-1584824
- Katzengold R, Topaz M, Gefen A. Tissue loads applied by a novel medical device for closing large wounds. *J Tissue Viability.* 2016;25(1):32-40. doi:10.1016/j.jtv.2015.12.003
- Katzengold R, Topaz M, Gefen A. Dynamic computational simulations for evaluating tissue loads applied by regulated negative pressure-assisted wound therapy (RNPT) system for treating large wounds. *J Tissue Viability.* 2018;27(2):101-113. doi:10.1016/j.jtv.2017.10.004
- Orlov A, Gefen A. How influential is the stiffness of the foam dressing on soft tissue loads in negative pressure wound therapy? *Med Eng Phys.* 2021;89:33-41. doi:10.1016/j.medengphy.2021.02.001
- Zeybek B, Li S, Fernandez JW, Stapley S, Silberschmidt VV, Liu Y. Computational modelling of wounded tissue subject to negative pressure wound therapy following trans-femoral amputation. *Biomech Model Mechanobiol.* 2017;16(6):1819-1832. doi:10.1007/s10237-017-0921-7
- Wilkes RP, Kilpad DV, Zhao Y, Kazala R, McNulty A. Closed incision management with negative pressure wound therapy (CIM): biomechanics. *Surg Innov.* 2012;19(1):67-75. doi:10.1177/1553350611414920
- Loveluck J, Copeland T, Hill J, Hunt A, Martin R. Biomechanical modeling of the forces applied to closed incisions during single-use negative pressure wound therapy. *Eplasty.* 2016;16:e20.
- Lustig A, Alves P, Call E, Santamaria N, Gefen A. The sorptivity and durability of gelling fibre dressings tested in a

- simulated sacral pressure ulcer system. *Int Wound J.* 2020;18:194-208. doi:10.1111/iwj.13515
27. Lustig A, Gefen A. Three-dimensional shape-conformation performances of wound dressings tested in a robotic sacral pressure ulcer phantom. *Int Wound J.* 2021;18:670-680. doi:10.1111/iwj.13569
  28. Lee Y, Hwang K. Skin thickness of Korean adults. *Surg Radiol Anat.* 2002;24(3-4):183-189. doi:10.1007/s00276-002-0034-5
  29. 3D Image Segmentation Software | Simpleware ScanIP. <https://www.synopsys.com/simpleware/software/scanip.html>. Accessed January 23, 2021.
  30. Hendriks FM, Brokken D, Oomens CWJ, Bader DL, Baaijens FPT. The relative contributions of different skin layers to the mechanical behavior of human skin in vivo using suction experiments. *Med Eng Phys.* 2006;28(3):259-266. doi:10.1016/j.medengphy.2005.07.001
  31. Xu F, Lu TJ. Chapter 3 skin biothermomechanics: modeling and experimental characterization. *Adv Appl Mech.* 2009;43:147-248. doi:10.1016/S0065-2156(09)43003-5
  32. Greenwald D, Shumway S, Albear P, Gottlieb L. Mechanical comparison of 10 suture materials before and after in vivo incubation. *J Surg Res.* 1994;56:372-377.
  33. Joshi CJ, Hsieh J-C, Hassan A, Galiano RD. Application of negative pressure wound therapy on closed incisions. *Wound Healing IntechOpen.* 2020. 10.5772/intechopen.88658
  34. Stannard JP, Robinson JT, Anderson ER, McGwin G, Volgas DA, Alonso JE. Negative pressure wound therapy to treat hematomas and surgical incisions following high-energy trauma. *J Trauma Inj Infect Crit Care.* 2006;60(6):1301-1306. doi:10.1097/O1.ta.0000195996.73186.2e
  35. Scherer LA, Shiver S, Chang M, Wayne Meredith J, Owings JT. The vacuum assisted closure device: a method of securing skin grafts and improving graft survival. *Arch Surg.* 2002;137(8):930-934. doi:10.1001/archsurg.137.8.930
  36. Gustafsson RI, Sjögren J, Ingemansson R. Deep sternal wound infection: a sternal-sparing technique with vacuum-assisted closure therapy. *Ann Thorac Surg.* 2003;76(6):2048-2053. doi:10.1016/S0003-4975(03)01337-7
  37. Runkel N, Krug E, Berg L, et al. Evidence-based recommendations for the use of negative pressure wound therapy in traumatic wounds and reconstructive surgery: steps towards an international consensus. *Injury.* 2011;42(SUPPL.1):S1-S12. doi:10.1016/S0020-1383(11)00041-6
  38. Matsumoto T, Parekh SG. Use of negative pressure wound therapy on closed surgical incision after total ankle arthroplasty. *Foot Ankle Int.* 2015;36(7):787-794. doi:10.1177/1071100715574934
  39. Emmerson AM, Enstone JE, Griffin M, Kelsey MC, Smyth ETM. The second National Prevalence Survey of infection in hospitals - overview of the results. *J Hosp Infect.* 1996;32(3):175-190. doi:10.1016/S0195-6701(96)90144-9
  40. Reilly J, Twaddley S, McIntosh J, Kean L. An economic analysis of surgical wound infection. *J Hosp Infect.* 2001;49(4):245-249. doi:10.1053/jhin.2001.1086
  41. Pellino G, Sciaudone G, Candilio G, Campitiello F, Selvaggi F, Canonico S. Effects of a new pocket device for negative pressure wound therapy on surgical wounds of patients affected with Crohn's disease: a pilot trial. *Surg Innov.* 2014;21(2):204-212. doi:10.1177/1553350613496906
  42. Baharestani M, Amjad I, Bookout K, et al. V.A.C.<sup>®</sup> therapy in the management of paediatric wounds: clinical review and experience. *Int Wound J.* 2009;6(SUPPL. 1):1-26. doi:10.1111/j.1742-481X.2009.00607.x
  43. Gleeson L. Using a portable, multi-week single-patient use negative pressure wound therapy device to facilitate faster discharge. *Wounds UK.* 2015;11:104-111.
  44. Sandy-Hodgetts K, Watts R. Effectiveness of negative pressure wound therapy/closed incision management in the prevention of post-surgical wound complications: a systematic review and meta-analysis. *JBIS Database System Rev Implement Rep.* 2015;13(1):253-303. doi:10.11124/jbisrir-2015-1687
  45. Scalise A, Calamita R, Tartaglione C, et al. Improving wound healing and preventing surgical site complications of closed surgical incisions: a possible role of incisional negative pressure wound therapy. A systematic review of the literature. *Int Wound J.* 2016;13(6):1260-1281. doi:10.1111/iwj.12492
  46. Norman G, Goh EL, Dumville JC, et al. Negative pressure wound therapy for surgical wounds healing by primary closure. *Cochrane Database Syst Rev.* 2020;5(5):CD009261. doi:10.1002/14651858.CD009261.pub5
  47. Shiroky J, Lillie E, Muaddi H, Sevigny M, Choi WJ, Karanicolas PJ. The impact of negative pressure wound therapy for closed surgical incisions on surgical site infection: a systematic review and meta-analysis. *Surgery.* 2020;167(6):1001-1009. doi:10.1016/j.surg.2020.01.018
  48. Hyldig N, Birke-Sorensen H, Kruse M, et al. Meta-analysis of negative-pressure wound therapy for closed surgical incisions. *Br J Surg.* 2013;103:477-486. doi:10.1002/bjs.10084
  49. Chen X, Li J, Li J, et al. Spatial-temporal changes of mechanical microenvironment in skin wounds during negative pressure wound therapy. *ACS Biomater Sci Eng.* 2019;5(4):1762-1770. doi:10.1021/acsbomaterials.8b01554
  50. Gefen A. Pressure-sensing devices for assessment of soft tissue loading under bony prominences: technological concepts and clinical utilization. *Wounds\*\*\*\*.* 2007;19(12):350-362.
  51. Birke-Sorensen H, Malmsjö M, Rome P, et al. Evidence-based recommendations for negative pressure wound therapy: treatment variables (pressure levels, wound filler and contact layer) - steps towards an international consensus. *J Plast Reconstr Aesthet Surg.* 2011;64(SUPPL. 1):S1-S16. doi:10.1016/J.BJPS.2011.06.001
  52. Borgquist O, Ingemansson R, Malmsjö M. The influence of low and high pressure levels during negative-pressure wound therapy on wound contraction and fluid evacuation. *Plast Reconstr Surg.* 2011;127(2):551-559. doi:10.1097/PRS.0B013E3181FED52A
  53. Timmers MS, Le Cessie S, Banwell P, Jukema GN. The effects of varying degrees of pressure delivered by negative-pressure wound therapy on skin perfusion. *Ann Plast Surg.* 2005;55(6):665-671. doi:10.1097/O1.SAP.0000187182.90907.3D
  54. Kairinos N, Voogd AM, Botha PH, et al. Negative-pressure wound therapy II: negative-pressure wound therapy and increased perfusion. Just an illusion? *Plast Reconstr Surg.* 2009;123(2):601-612. doi:10.1097/PRS.0B013E318196B97B
  55. Lear W, Roybal LL, Krucic JJ. Forces on sutures when closing excisional wounds using the rule of halves. *Clin Biomech.* 2020;72:161-163. doi:10.1016/J.CLINBIOMECH.2019.12.018

56. Kazmer DO, Eaves FF. Force modulating tissue bridges for reduction of tension and scar: finite element and image analysis of preclinical incisional and nonincisional models. *Aesthet Surg J*. 2018;38(11):1250-1263. doi:10.1093/ASJ/SJY079
57. Pitts J. Skin perfusion pressure: a case study demonstrating microcirculatory blood flow. *J Diagn Med Sonogr*. 2014;30(4):213-216. doi:10.1177/8756479314532714
58. Palevski A, Glaich I, Portnoy S, Linder-Ganz E, Gefen A. Stress relaxation of porcine gluteus muscle subjected to sudden transverse deformation as related to pressure sore modeling. *J Biomech Eng*. 2006;128(5):782-787. doi:10.1115/1.2264395
59. Gefen A, Haberman E. Viscoelastic properties of ovine adipose tissue covering the gluteus muscles. *J Biomech Eng*. 2007;129(6):924-930. doi:10.1115/1.2800830
60. SIMULIA User Assistance. Hyperelastic behavior of rubberlike materials. 2020. [https://help.3ds.com/2020/english/dssimulia\\_established/simacaematrefmap/simamat-c-hyperelastic.htm?contextscope=all](https://help.3ds.com/2020/english/dssimulia_established/simacaematrefmap/simamat-c-hyperelastic.htm?contextscope=all). Accessed January 26, 2021.
61. SIMULIA User Assistance. Time domain viscoelasticity. 2020. [https://help.3ds.com/2020/english/dssimulia\\_established/simacaematrefmap/simamat-c-timevisco.htm?contextscope=all](https://help.3ds.com/2020/english/dssimulia_established/simacaematrefmap/simamat-c-timevisco.htm?contextscope=all). Accessed January 26, 2021.
62. D3574-11 AITS. Standard test methods for flexible cellular materials - Slab, Bonded, and molded urethane foams. *Am Soc Test Mater*. 2012. 1-29. [10.1520/D3574-11.2](https://doi.org/10.1520/D3574-11.2)
63. Portnoy S, Vuillerme N, Payan Y, Gefen A. Clinically oriented real-time monitoring of the individual's risk for deep tissue injury. *Med Biol Eng Comput*. 2011;49(4):473-483. doi:10.1007/S11517-011-0754-Y

**How to cite this article:** Orlov A, Gefen A. The potential of a canister-based single-use negative-pressure wound therapy system delivering a greater and continuous absolute pressure level to facilitate better surgical wound care. *Int Wound J*. 2022;19(6):1471-1493. doi:10.1111/iwj.13744

## APPENDIX A.

### A.1. | Mechanical behaviour and properties of the model components

Each of the aforementioned soft tissues was assumed to behave as a viscoelastic solid. The hyperelastic component of this viscoelastic behaviour was considered as Neo-Hookean<sup>21,30,60</sup> with a strain energy density function  $W$ :

$$W = C_{10}(\bar{I}_1 - 3) + \frac{1}{D_1}(J - 1)^2, \quad (\text{A1})$$

where  $C_{10}$  and  $D_1$  are material-specific parameters, respectively,  $I_1$  is the first invariant of the right Cauchy-Green deformation tensor and  $J$  is the determinant of the

deformation gradient tensor ( $F$ ). The viscous (stress relaxation) component of the viscoelastic behaviour of each soft tissue type was simulated using a Prony-series<sup>61</sup>:

$$g_R(t) = 1 - \sum_{i=1}^N g_i^P \left(1 - e^{-t/\tau_i^G}\right), \quad (\text{A2})$$

where  $g_i^P$ ,  $\tau_i^G$  and  $i = 1, 2, \dots, N$ , are the tissue-specific material constants. For efficiency of the numerical computations and to minimise the number of parameters, we selected  $N = 2$  (Equation [A2]), which yields short-term and long-term viscoelastic relaxation time constants for each soft tissue type,  $\tau_1$  and  $\tau_2$ , respectively. The  $C_{10}$  and  $D_1$ ,  $\tau_1$  and  $\tau_2$  and  $g_1$  and  $g_2$  parameter values for each tissue type were selected based on the published literature as detailed in Table 2. The sutures were modelled as linear elastic with properties of nylon that are likewise provided in Table 2.<sup>20,32</sup>

To determine the mechanical properties of the NPWT dressings in the dry state vs when subjected to the simulated wound fluid, we conducted experimental testing on each of the suNPWT dressings (used with either the CB-125 or the CL-80 suNPWT systems), by means of an electromechanical material testing machine (Instron Series 5944, Instron Co., Norwood, Massachusetts). The dressing specimens were tested in a compressive loading mode according to the relevant testing standard ASTM D3574-11,<sup>62</sup> using a deformation rate of  $50 \pm 5$  mm/min. The effect of exudate absorption in the dressing on its compressive stiffness was considered in these tests, by submerging the samples for 5 minutes in a non-biological, viscous exudate-like fluid developed in our laboratory.<sup>26</sup> This exudate-like fluid contained food-standard Xanthan gum powder at a concentration of 0.01% that has been mixed in distilled water.<sup>26</sup> The viscosity of the aforementioned fluid was pre-calibrated through testing in a rheometer (model AR-G2, TA instruments, New Castle, Delaware) and was found to be  $0.006 \text{ Pa} \times \text{s}$  at room temperature, corresponding to the real-world exudates of surgical wounds.<sup>26</sup> A total of six specimens were tested for each dressing type (of the CB-125 vs the CL-80 suNPWT systems), separately for the dry dressings and the dressings exposed to the fluid, and corresponding compressive stress-strain curves were obtained (Figure 4). Considering the specimens of both the dry dressing and the dressing managing the fluid as homogenous, isotropic and hyperelastic materials, we have used the ABAQUS software suite (ver. 2020, Dassault Systems Simulia Corp., Johnston, Rhode Island) to determine their  $C_{10}$  and  $D_1$  parameter values using a computational 'reverse engineering' material property calibration process. These mechanical properties of the dressings, reported in



Table 2, were further used to obtain the computational results that are reported here.

## A.2. | Stress-dose calculations

In our historical research, focussing on the aetiology of pressure ulcers/injuries and diabetic foot ulcers, we have used the concept and term ‘stress-dose’ (or its equivalent for surface loads, which is the ‘pressure-dose’), to indicate the extent of tissue exposure to a (potentially varying) loading state over time. This approach, of referring to a stress-dose, is fundamentally different from the determination of a ‘snapshot’ of a skin stress datum in time, that is, a momentary stress level which does not consider the sustained and continuous skin exposure to the stress concentrations around sutures, which is studied here (Figure 5). We further demonstrated that the stress-dose is an adequate biomechanical measure and a clinically oriented, intuitive indicator of the cumulative soft tissue exposure to mechanical stresses over time.<sup>63</sup>

Further to the above, a stress-dose difference (SDD) between the two suNPWT systems subjected to this study was defined here, as  $\Delta\sigma \times t$ , where  $\Delta\sigma$  is the difference between the stress concentration levels around the sutures for the two suNPWT system types. However, if considering that the dressing of the CL suNPWT system gradually accumulates fluids over the course of the treatment time  $T$ , thereby increasing the likelihood of loss of therapy effectiveness (ie, occurrence of pressure drops) as demonstrated in Figure 2A,B, the simple aforementioned definition of the SDD, that is,  $\Delta\sigma \times t$ , does not hold true anymore. That is, if the CL suNPWT system is in fact fluctuating in its negative-pressure levels, so that  $\Delta\sigma$  also depends on the time  $t$ , then the definition of the SDD becomes:

$$\text{SDD} = \int_0^T \Delta\sigma(t) dt. \quad (\text{A3})$$

Moreover, if the CL-80 suNPWT system does not deliver the  $|-80|$  mmHg pressure level in practice, but, based on

the data in Figure 2A,B, gradually drops to  $|-60|$  mmHg (or lower) over the treatment period  $T$ , then the difference in the stress concentration levels around the sutures  $\Delta\sigma(t)$  will increase correspondingly. For example, the difference in the tissue stress concentration levels around the sutures between the two suNPWT system types may increase linearly, as  $\Delta\sigma(t) = \Delta\sigma_0(1 + \frac{\alpha t}{T})$ , where  $\Delta\sigma_0$  is the initial %-difference in the stress concentration levels around the sutures at the time of application of the two suNPWT systems and  $\alpha$  is the slope of the increase of the aforementioned stress difference over time  $t$  during the period of treatment  $T$ . In the above example, a linear decay in the level of the pressure delivered by the CL suNPWT system yields that the SDD increases non-linearly over time, due to an added quadratic term, as follows:

$$\text{SDD} = \int_0^T \Delta\sigma(t) dt = \int_0^T \Delta\sigma_0 \left(1 + \frac{\alpha t}{T}\right) dt = \Delta\sigma_0 \left(t + \frac{\alpha t^2}{2T}\right). \quad (\text{A4})$$

Similarly, if the decay in the level of pressure is exponentially plateauing as in Figure 2A, then:

$$\begin{aligned} \text{SDD} &= \int_0^T \Delta\sigma(t) dt = \int_0^T \left[ \Delta\sigma_0 + \beta \Delta\sigma_0 \left(1 - e^{-\frac{\gamma t}{T}}\right) \right] dt \\ &= \Delta\sigma_0 \left[ (1 + \beta)t + \beta \frac{T}{\gamma} \left(e^{-\frac{\gamma}{T}} - 1\right) \right] \end{aligned} \quad (\text{A5})$$

where  $\beta$  and  $\gamma$  are constants characterising the corresponding exponentially plateauing behaviour of the difference in the skin stress levels around the sutures between the two suNPWT system types. In the above case, again, a non-linear time-dependent term has been added to the SDD, due to the loss of the negative-pressure level demonstrated by the CL suNPWT system.